Contributed Papers on other Topics

Experiences of the BKG in Processing GLONASS and Combined GLONASS/GPS Observations

Heinz Habrich
Federal Agency for Cartography and Geodesy
D-60598 Frankfurt Main, Germany

Abstract

The Global Navigation Satellite System (GLONASS) is operated by the Russian Space Forces, Ministry of Defence of the Russian Federation. The satellite's constellation and the signal in space of both GLONASS and GPS are comparable. This enables a geodetic usage of GLONASS with the availability of a 48 satellites constellation in the case of a combination of GLONASS and GPS observations.

A joint effort of the Astronomical Institute of Beme (AIUB) and the Federal Agency for Cartography and Geodesy (BKG, former Institute of Applied Geodesy) has been established to modify the Bernese GPS Software for the processing of GLONASS and combined GLONASS/GPS observations. The reference system and the system time for GLONASS are different from the corresponding GPS quantities and have to be considered. New algorithms for ambiguity resolution and cycle slip detection are used to account for the satellite-specific GLONASS frequencies. The BKG has processed GLONASS and combined GLONASS/GPS phase observations. The performed processing steps include the generation of combined GLONASS/GPS orbit files, cycle slip corrections and the resolution of the carrier phase ambiguities.

Introduction

GLONASS observations can be processed similarly to GPS, provided two basic characteristics are taken into consideration: (1) The broadcast satellite's positions refer to the PZ-90 reference frame and the system time is synchronized to UTC(Moscow). (2) GLONASS satellites transmit it's signal on satellite-specific frequencies. The first item is of importance for the combined processing of GLONASS and GPS observations. Orbit files must refer to a unique reference frame and the GLONASS system time has to be transformed to GPS time. At BKG combined orbit files in the SP3-format are generated. The second item has to be modelled carefully in the carrier phase observation equations.

The double difference observations show a new bias term, which effects the integer ambiguity parameters and the cycle slip detection.

The new ambiguity resolution algorithm solves successively for the integer ambiguities. Therefore the effect of the new bias term on the ambiguities is reduced to a minimum. In order to assign cycle slips to the correct satellites, a new iterative approach is used. Cycle slips detected by triple differences are applied to the correct single difference. New ambiguities are introduced, if cycle slips can not be assigned to a single satellite. The ***new*** approaches for ambiguity resolution and cycle slip correction can be used for GLONASS and GPS or combined GLONASS/GPS observations.

The BKG is operating a permanent GLONASS/GPS receiver at it's Fundamental Station Wettzell. Recorded observations are available in the RINEX format.

Generation of Combined GLONASS/GPS Orbits

In order to process combined GLONASS/GPS observations an orbit file containing navigation messages of both GLONASS and GPS satellites has to be generated. Table 1 shows differences of the two systems which are most relevant for a combination.

	GLONASS	**GPS**
Reference System	PZ-90	WGS-84
System Time	GLONASS time, UTC - GLONASS <1 μsec (since July 1, 1997)	GPS time, GPS - UTC = 12 sec (January 1998)
Broadcast Ephemerides	satellite's position, velocity and acceleration, every 15 and 45 min	modified Kepler elements, every full hour
Carrier Frequency	L1 :1602 + k* O.5625 MHz L2: 1246+ k* 0.4375 MHz ,k=1,2,...,24	Ll: 1575.42 MHz L2: 1227.60 MHz

Table 1: GLONASS/GPS System Differences

A combined orbit file in the WGS-84 reference system, referred to the GPS time scale, can be generated in the SP3-format. The required transformations are shown in Figure 1, supporting the existence of both GLONASS and GPS RINEX navigation files. Concerning GLONASS, the RINEX format has currently been extended [Gurtner, 1997]. GPS position coordinates for the SP3-file epochs are calculated from Kepler elements. Epochs of the GLONASS navigation data are transferred to GPS time through adding an integer number of seconds (e.g. 12 sec for January 1998). The position, velocity and

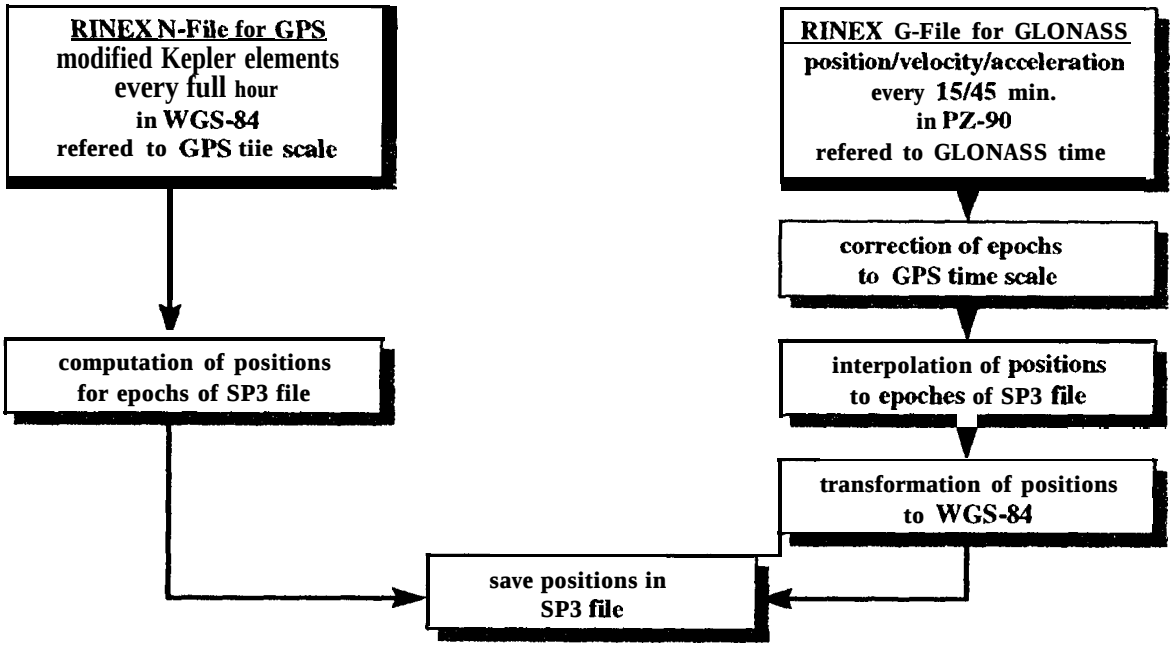

Figure 1: Generation of Combined SP3-Orbit Files

acceleration of the GLONASS satellites are given for the epochs of the broadcast ephemerides and used to compute the position for the SP3-file epochs. For the interpolation of positions we use formulas according to [ICD, 1995] within a time interval of 15 min. These formulas are given in Table 2 and account for the

- central part of Earth's **gravitational potential,**
- zonal geopotential **effects characterized by C_{20},**
- **approximate transformation between celestial and terrestrial coordinate system,**
- **accelerations caused by** sun and **moon,**

The Runge-Kutta method can be used for the necessary numerical integrations. Figure 2

$$\ddot{x} = -\frac{\mu}{r^3}\cdot x + \frac{3}{2}\cdot C_{20}\cdot\frac{\mu\cdot a^2}{r^5}\cdot x\left(1-\frac{5\cdot z^2}{r^2}\right) + \omega^2\cdot x + 2\cdot\omega\cdot\dot{y} + \ddot{X}$$

$$\ddot{y} = -\frac{\mu}{r^3}\cdot y + \frac{3}{2}\cdot C_{20}\cdot\frac{\mu\cdot a^2}{r^5}\cdot y\left(1-\frac{5\cdot z^2}{r^2}\right) + \omega^2\cdot y - 2\cdot\omega\cdot\dot{x} + \ddot{Y}$$

$$\ddot{z} = -\frac{\mu}{r^3}\cdot z + \frac{3}{2}\cdot C_{20}\cdot\frac{\mu\cdot a^2}{r^5}\cdot z\left(3-\frac{5\cdot z^2}{r^2}\right) + \ddot{Z}$$

Table 2: Approximate Equation of Motion for GLONASS Satellites

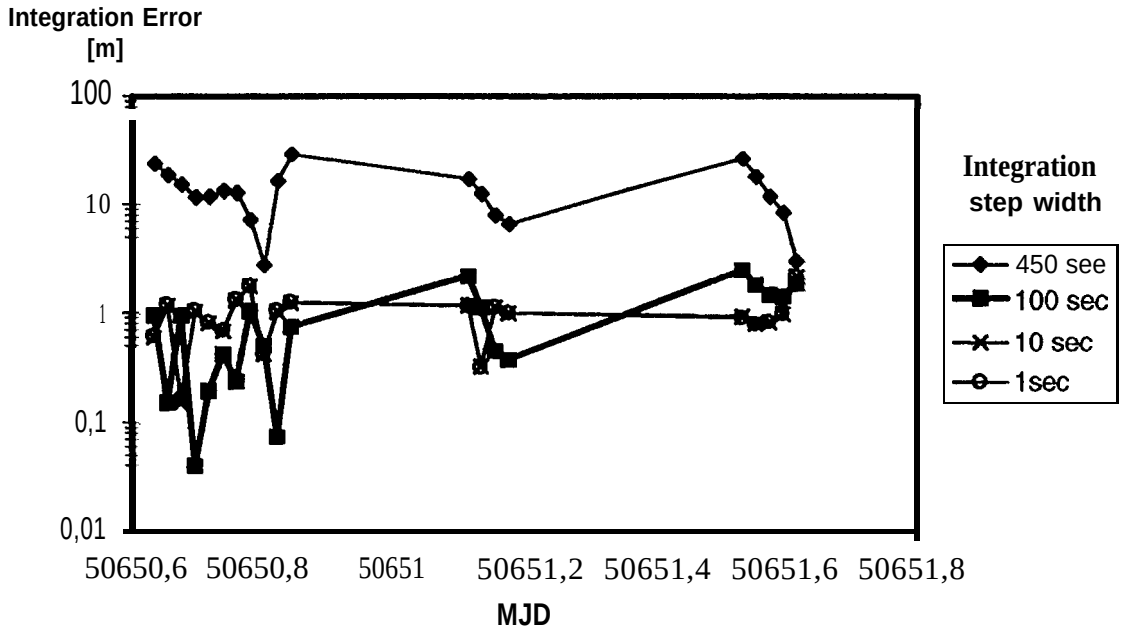

Figure 2: Numerical Integration error for X-Component, 15 rnin intervals

shows the discrepancies between a forward integration for the X-component (initial value is the broadcast position for epoch *i)* and a backward integration (initial value is the broadcast position for epoch ***i*** + 30 ***rein)*** for the epoch *i* + ***15 min***, using four different integration step widths (450, 100, 10 and 1 see). The 10 sec and 1 sec integration step width lead to nearly identical results.

The GLONASS satellite positions are transformed from PZ-90 to WGS-84 and then stored in the SP3-format. Two sets of approximate transformation parameters have been estimated in 1996 as given in Table 3.

$\begin{bmatrix} x \\ y \\ z \end{bmatrix}_{WGS-84} = \begin{bmatrix} 1 & -0.33'' & 0 \\ 0.33'' & 1 & 0 \\ 0 & 0 & 1 \end{bmatrix} \cdot \begin{bmatrix} u \\ v \\ w \end{bmatrix}_{PZ-90}$	Roßbach et al. 1996 Post-fit residuals: 30 - 40 cm
$\begin{bmatrix} x \\ y \\ z \end{bmatrix}_{WCS-84} = \begin{bmatrix} 0 \\ 2.5m \\ 0 \end{bmatrix} + \begin{bmatrix} 1 & -0.39'' & 0 \\ 0.39'' & 1 & 0 \\ 0 & 0 & 1 \end{bmatrix} \cdot \begin{bmatrix} u \\ v \\ w \end{bmatrix}_{PZ-90}$	Misra et al. 1996 Post-fit residuals: 1 - 30 m

Table 3: Transformation Parameters, PZ-90 to WGS-84

The combined SP3-file includes also clock corrections for GLONASS and GPS satellites. Clock and frequency corrections are transmitted by the GLONASS satellites and are used to compute the satellite clock correction for the SP3-file epochs.

Phase Observable

The satellite specific frequencies (resp. wavelengths) have to be modelled correctly for the phase observable. This leads to the following observation equations:

Zero Difference Observable

$$\Psi_k^i = c \cdot \tau_k^i + N_k^i \cdot \lambda^i + c \cdot \Delta t_k - c \cdot \Delta t^i$$

where

c	=	Velocity of light
τ_k^i	=	Signal travel time between satellite i and receiver k, including the tropospheric and ionospheric bias
N_k^i	=	Unknown integer number of cycles (ambiguity)
λ^i	=	Nominal wavelength of signal from satellite i
At^i	=	Satellite clock error at time of emission
At_k	=	Receiver clock error at time of reception

Single Difference Phase Observable

$$\Delta\Psi_{kl}^i = c \cdot \Delta\tau_{kl}^i + N_{kl}^i \cdot \lambda^i + c \cdot \Delta t_{kl}$$

where

$$\Delta\tau_{kl}^i = \tau_k^i - \tau_l^i$$
$$N_{kl}^i = N_k^i - N_l^i$$
$$\Delta t_{kl} = t_k - t_l$$

Double Difference Phase Observable

$$\Delta\Delta\Psi_{kl}^{ij} = c \cdot \Delta\Delta\tau_{kl}^{ij} + N_{kl}^{ij} \cdot \lambda^i + N_{kl}^j \cdot \Delta\lambda^{ij}$$

where

$$\Delta\Delta\tau_{kl}^{ij} = \Delta\tau_{kl}^i - \Delta\tau_{kl}^j$$
$$\Delta\lambda^{ij} = \lambda^i - \lambda^j$$
$$N_{kl}^{ij} = N_{kl}^i - N_{kl}^j$$

The double differences show the new bias term $b^{ij} = N_{kl}^{j} . \Delta\lambda^{ij}$ which

- destroys the **integer nature of the ambiguities,**
- **. depends on the wavelength differences of the two satellites**
- **. needs single difference ambiguities N_{kl}^{j} to be known.**

The integer ambiguities may be found, if the bias term is smaller than 0.1 cycles. This is true for small wavelength differences of the two satellites or if the single difference ambiguities are known with an accuracy of a few cycles. Table 4 shows examples in units of the reference wavelength λ_0.

	$\Delta\lambda$ [cycles of λ_0]	**maximum allowed N_{kl}^{j} for $b_{ij} \leq 0.1$** [cycles of λ_0]
GLONASS-GLONASS (rein)	**0.0035**	**285**
GLONASS-GLONASS (max)	**0.0081**	**12**
GPS-GLONASS (max)	**0.0253**	**4**

Table 4: Numerical Values for Single Difference Bias Term

For the minimum wavelength difference for two GLONASS satellites the single difference ambiguities N_{kl}^{j} have to be known within an accuracy of 285 cycles which is possible, e.g. after computing a Code single point positioning.

Ambiguity Resolution

The single difference bias term causes problems for the ambiguity resolution. With the assumption, that the singe difference ambiguities N_{kl}^{j} are known with an accuracy of e.g. 200 cycles, we can resolve the ambiguities of satellite pairs with small wavelength differences, but not for those with larger wavelength differences (see Table 4). To overcome this problem, an iterative approach is used.

The ambiguities of satellite pairs with small wavelength differences are solved first. The following iterations show significant smaller RMS errors for the single difference ambiguities and allow the ambiguity resolution for satellite pairs with larger wavelength difference. The ambiguity resolution algorithm can be summarised to six steps as given in Table 5.

The RMS errors for double difference ambiguities as computed in step 3) of Table 5 are given in Figure 3; the RMS errors depend on the wavelength difference of the two satellites. Due to the single difference bias term, for small wavelength differences the double difference ambiguities can be fixed to an integer number with the frost iteration. The rectangular symbols show the RMS errors of the corresponding iteration step, when the ambiguities were fixed to an integer. Due to the iterative procedure, even for large wavelength differences the RMS values are smaller than 0.1 cycles.

1) Set up ***n* single difference ambiguities N_{kl}^{j} for *n* satellites as unknown parameters (singular).**

→ **2) Introduce a priori constraint for N_{kl}^{j} (e.g. 300 cycles) and compute first solution vector with covariance matrix.**

3) Compute all possible double difference ambiguities N_{kl}^{jj} and the corresponding formal errors (integer destroyed by bias term).

4) Fix the best determined double difference ambiguity to an integer number.

5) Eliminate one single difference ambiguity from the normal equation system .If $\Delta\lambda \neq$ O:

a) Normal equation system is now regular.

b) RMS error of N_{kl}^{j} decreases significantly in next iteration.

Next iteration, (n-1) single difference ambiguities N_{kl}^{j} may be eliminated.

6) Estimate the unresolved N_{kl}^{j} as real value in the final solution.

Table 5: Ambiguity Resolution Approach

Figure 4 shows the RMS errors of the single difference ambiguities as computed in each iteration step. In each of the first eleven iterations one ambiguity between two GPS satellites (identical wavelength) has been resolved. This does not improve the RMS error. In the twelfth iteration step the wavelength difference of the corresponding satellite pair was not equal zero, leading to a decreased RMS error for the single difference ambiguities.

Figure 5 shows the fractional parts of the ambiguities, solved for pairs of two GPS satellites, two GLONASS satellites and a GPS/GLONASS satellite pair.

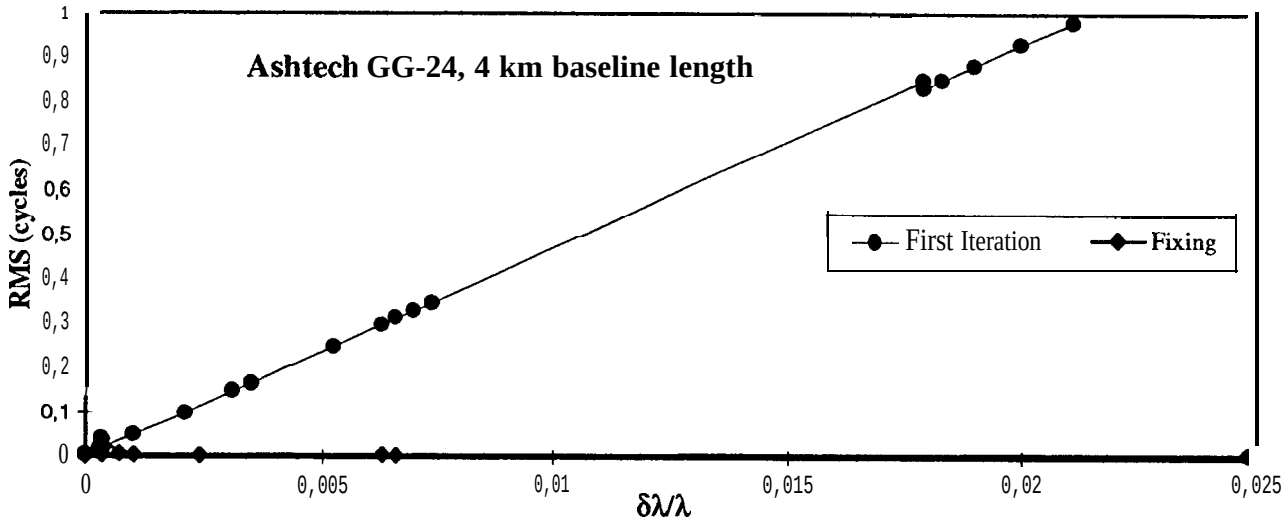

Figure 3: RMS Error of Double Difference Ambiguities

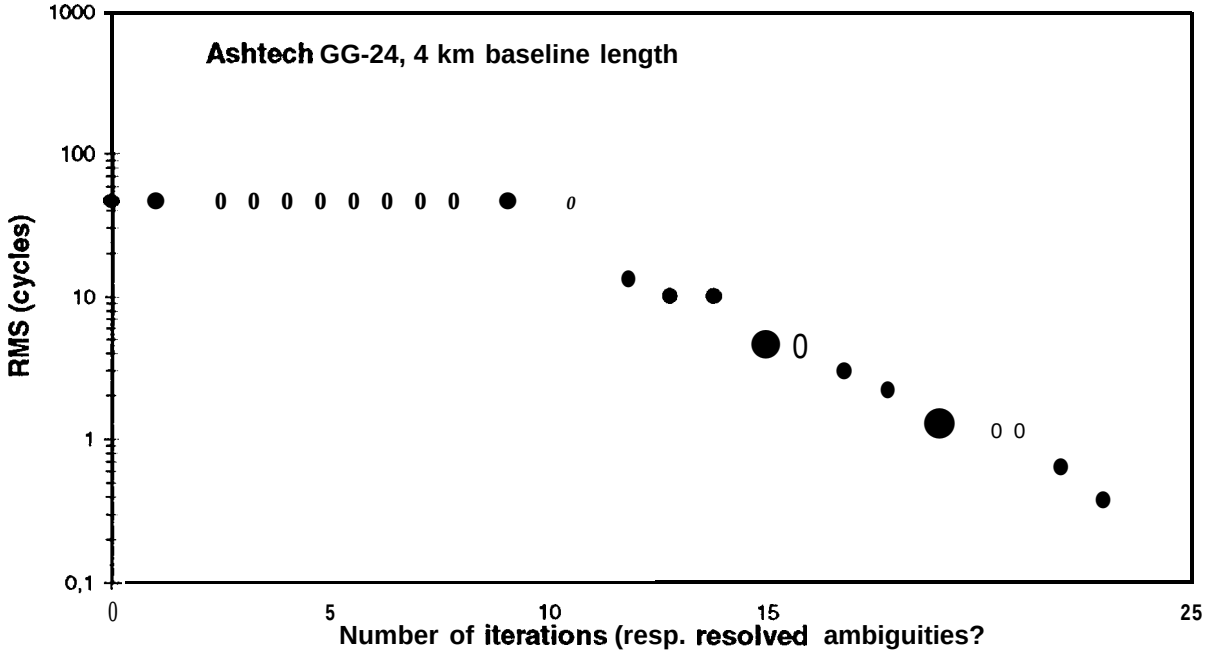

Figure 4: RMS Error of Single Difference Ambiguities

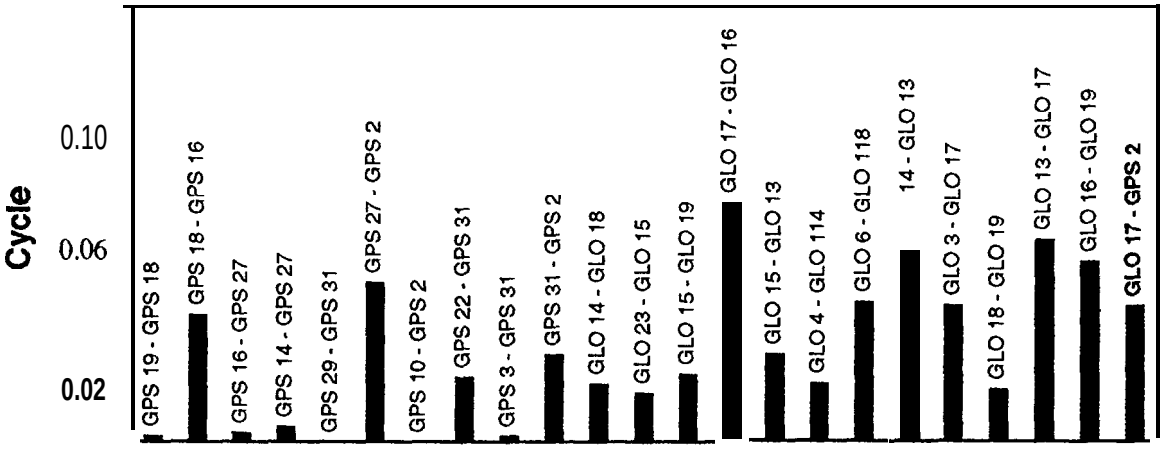

Figure 5: Fractional Parts of Resolved Ambiguities

Cycle Slip Detection

Two general qualities characterise the cycle slip detection for satellite specific frequencies:

- A Cycle slip has to be assigned to the responsible involved satellite, i.e. applied to the correct single difference.
- New ambiguities have to be introduced for cycle slips, which can not be assigned to a specific satellite.

In order to detect cycle slips, the triple difference residuals can be interpreted as

$$\Delta\Delta\Delta r_{kl}^{ij}(t_2 - t_1) = b_i \cdot \lambda^i - b_j \cdot \lambda^j$$

with

$$b_i = N_{kl}^i(t_2) - N_{kl}^i(t_1)$$
$$b_j = N_{kl}^j(t_2) - N_{kl}^j(t_1).$$

The formulas above lead to following facts:

- Residuals are close to zero, if no cycle slip occurs.
- Residuals are singular for the determination of b_i **and** b_j.
- The difference $(b_i - b_j)$ ***can*** **not be determined, because** $\lambda^i - \lambda^j \neq 0$.
- The cycle slip can be assigned to a single satellite, as soon as b_i **or** b_j ***is*** known (i.e. equal zero).

Three examples for cycle slips and the corresponding triple difference residuals are given in Table 6. A cycle slip of size „one cycle" was assumed for satellite i (resp. j) in example 1 (resp. 2). This slips will be detected, but can not be assigned to a specific satellite, because the triple difference residuals are not significantly different ($\Delta\lambda^{ij}$ is small compared to λ^i or λ^j). **The cycle slips assumed for example 3 may not be detected.**

Example	b_i	b_j	$\Delta\Delta\Delta r_{kl}^{ij}(t_2 - t_1)$
1	1	0	λ^i
2	o	-1	$\lambda^i - \Delta\lambda^{ij}$
3	1	1	$\Delta\lambda^{ij}$

Table 6: Cycle slips in triple difference residuals

In order to calculate the integer numbers of cycles for the single difference observation corrections, the triple difference residuals have to be converted into units of cycles. Figure 6 shows two alternative methods for this conversion.

The integer numbers are destroyed by a bias term in both cases. Besides the wavelength difference, the bias term depends on the size of the slip (first formula) or the relative receiver clock error (second formula). Using the second formula, one can reduce the influence of the bias term through an estimation of the receiver clock error.

A station ➡ A satellite ➡ A epoch ➡ [m ➤ cycles] :

$$\frac{\Delta\Delta\Delta r_{kl}^{ij}(t_2 - t_1)}{\lambda^i} = b_i - b_j + b_j \frac{\Delta\lambda}{\lambda^i}$$

❑ Bias term depends on size of slips

A station ➡ A epoch ➡ [m ➤ cycles] ➡ A satellite

$$\frac{\Delta\Delta r_{kl}^{i}(t_2 - t_1)}{\lambda^i} \frac{\Delta\Delta r_{kl}^{j}(t_2 - t_1)}{\lambda^j} = b_i - b_j - \frac{c \cdot \Delta\Delta t_{kl}(t_2 - t_1) \cdot \Delta\lambda}{\lambda^i \cdot \lambda^j}$$

❑ Bias term depends on receiver clock error changes

Figure 6: Triple Difference Residuals **in Units of Cycles, two approaches**

1) Compute triple difference residuals for all satellite pairs and select pairs with „no slip".
2) Find satellite pair with smallest $\Delta\lambda$ in all satellites with „no slip" and set $b_i=b_j=0$.
3) Find satellite pair „with slip" which includes one of the „clean" satellites and assign the cycle slip to the other satellite.
4) Correct cycle slip to the single difference observation and start next iteration.
5) Introduce new ambiguities for cycle slips which could not be assigned to a single satellite.

Table 7: Iterative Approach for Cycle Slip Correction

Obviously the bias term is smallest, for smallest wavelengths differences of the two satellites. This leads to an iterative approach for cycle slip correction. A scheme for this algorithm is given in Table 7.

GLONASS Permanent Station Wettzell

The BKG operates a combined GLONASS/GPS dual frequency receiver at the Fundamental Station in Wettzell on a permanent basis. The receiver of type 3S-Navigation R1OW4O has been installed in January 1996. Due to receiver failures an observation gap occurred in 1997. The receiver has been re-installed in January 1998 for a permanent tracking.

The receiver operates in the following mode:

. Up to 5 GLONASS satellites on L 1, C/A-code,
. up to 5 GPS satellites on L1, C/A-code,
• up to 8 GLONASS satellites on L2, P-code,
• 30 sec. measurement interval
. receiver clock synchronisation to UTC,
• time transfer mode enabled.

The observation and navigation data are available in the RINEX format from BKG's anonymous ftp-server <igs.ifag.de>.

Conclusion

It has been demonstrated, that GLONASS and combined GLONASS /GPS carrier phase observations can be processed. As a joint effort of AIUB and BKG, the Bernese GPS Software has been modified for the new requirements. Combined orbit files for GLONASS and GPS satellites were generated in the SP3-format. New approaches for ambiguity resolution and cycle slip detection were used, in order to take satellite specific frequencies into consideration. A satellite constellation of up to 48 satellites (combination of GLONASS and GPS) can be used for geodetic applications.

References

Gurtner W. (1997): *RINEX, The Receiver Independent Exchange Format Version 2 , updated revision,* Astronomical Institute University of Berne

ICD (1995): *GLONASS Interface Control Document,* Coordinational Scientific Information Center of Russian Space Forces, Moscow, Russia

Misra P. N., Abbot R. I., Gaposchkin E.M. (1996): *Transformation Between WGS-84 and PZ-90*, Proceedings of the 9* International Technical Meeting of the Satellite Division of the Institute of Navigation, ION GPS-96, Kansas City, Missouri

Roßbach U., Habrich H., Zarraoa N. (1996): *Transformation Parameters Between PZ-90 and WGS-84,* Proceedings of the 9th International Technical Meeting of the Satellite Division of the Institute of Navigation, ION GPS-96, Kansas City, Missouri

PRECISE AUTONOMOUS EPHEMERIS DETERMINATION FOR FUTURE NAVIGATION SATELLITES

Miguel.M. Romay-Merino, Patrick van Niftrik

GMV, Isaac Newton 11, P.T.M. Tres Cantos, E-28760 Madrid, Spain

ABSTRACT

Ephemeris errors are one of the major contributors to the total UERE (User Equivalent Range Error) budget. The user positioning accuracy can be determined as the product between the UERE and the DOP (Dilution of Precision). To minimise the total positioning errors accurate ephemeris shall be computed in real time. In this paper the different algorithms that can be used to compute accurate orbits in real time are presented. They can be classified in:

. On ground orbit determination algorithms

. On-board orbit determination algorithms

This paper will be focused on on-board or autonomous orbit determination algorithms. Results obtained using simulated data indicate that those techniques would be able to provide accurate ephemeris if accurate tracking data is available.

REAL TIME ORBIT DETERMINATION ALGORITHMS

Three types of algorithms can be considered for orbit determination:

1. Dynamic algorithms

2. Reduce dynamic algorithms

3. Geometric algorithms

Geometric algorithms are not able to provide the required accuracy for high orbiting satellites, therefore those algorithms will not be considered here.

Dynamic algorithms are based on the integration of the satellite motion equations. Very accurate dynamic models are currently available, therefore it would be possible to

compute high accurate orbits using this type of algorithms. Their major drawback is that they require a significant amount of computational time, so they are in principle not valid for real time applications. In the other hand these algorithms are able to compute accurate orbit predictions, so orbit predictions could be used to compute in real time the ephemeris message to be sent to the user. This technique is schematically represented in the following figure:

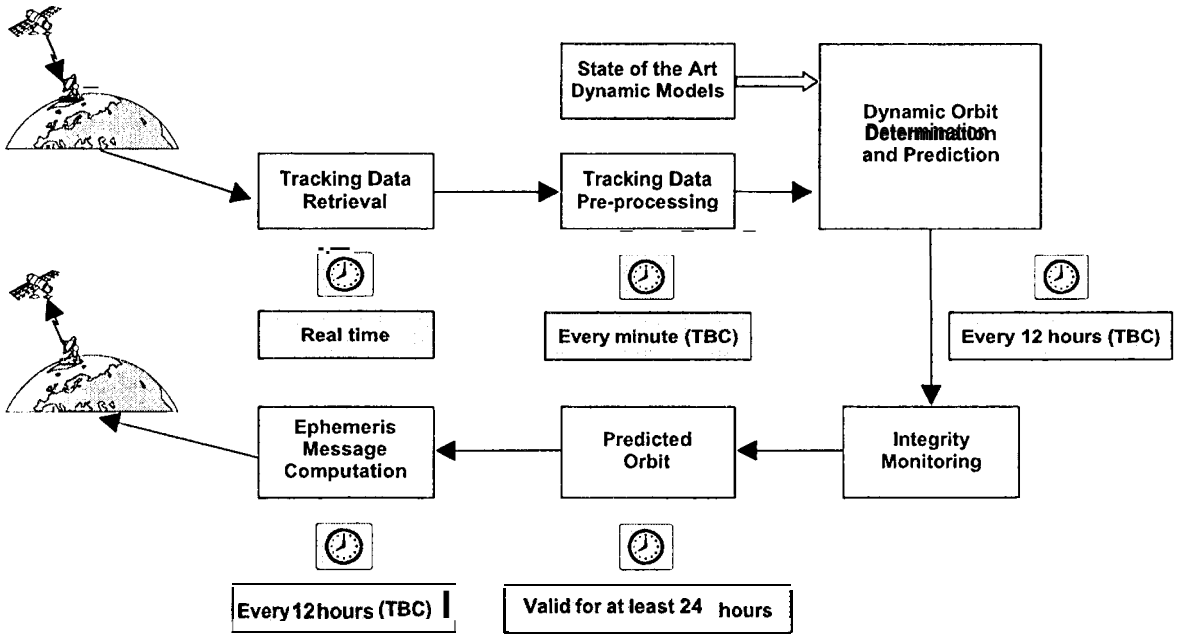

Figure 1 Schematic representation of a real time dynamic orbit determination algorithm

The tracking data is collected at the different ground stations and it is sent in real time to the MMCC (Mission Management Control Centre). At the MMCC the tracking data is retrieved and pre-processed shortly after the arrival. At regular time intervals (i.e. every 12 hours) the orbit determination program runs, and after an integrity check a new orbit prediction will be available. This orbit prediction will be valid for the next hours (for high orbiting satellites at least 24 hours), a very simple orbit model will be fitted to the predicted orbit, and the parameters of this model will be sent to the users (ephemeris message). With the ephemeris message the users will be able to determine the position of any satellite in the constellation at any epoch with the desired accuracy.

This technique requires to send the data to the MMCC, there a heavy processing is required, and then the ephemeris message has to be sent to the satellite, and finally the satellite will send back the ephemeris message to the users.

This scheme can be severely simplified if two way measurements (satellite-ground station-satellite) are considered, then the processing can be done on-board, where also the

ephemeris message will be computed and finally this message will be send to the users. If the integrity monitoring could also be done on-board the MMCC will not be responsible for any orbit determination activity.

This technique is schematically represented in the following figure:

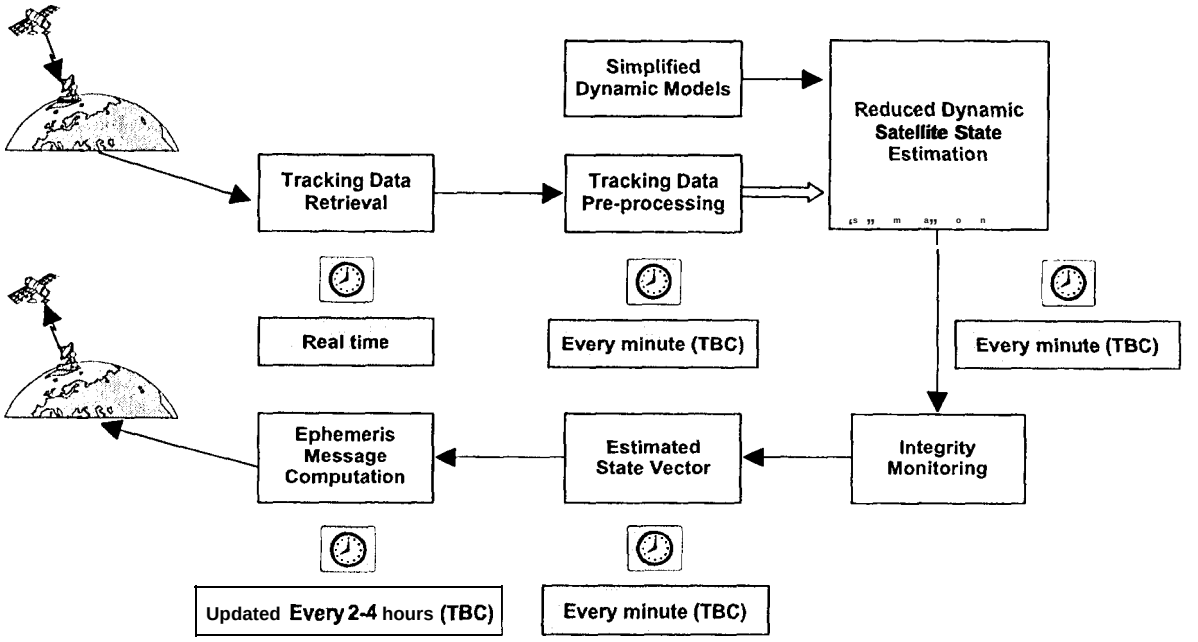

Figure 2 Schematic representation of a real time reduced dynamic orbit determination algorithm

This type of algorithms are only able to work in real time if the reduce dynamic algorithm is able to accomplish some very stringent requirements, like:

. Low computational loads

. Real time

. Accuracy

• Integrity

The core of the proposed strategy is the estimation module. The estimation module which is proposed is a least squares algorithm including measurement's weight and a priori information. It can be demonstrated that this algorithm can be equivalent to a classical batch least squares algorithm, but also to a Kalman filter. The different parameters of the filter can be adjusted in order to have a classical batch, or a Kalman filter, or an intermediate algorithm. Most of the already existing on-board orbit determination packages are based in the use of Kalman filters, while most of the on-

ground orbit determination algorithms are based in the use of least squares batch algorithms. Both algorithms have some advantages and drawbacks:

- The major advantage of the least squares batch algorithms is their robustness, this is very important for an on board GNSS orbit determination where stringent integrity requirements are imposed. The major drawback of the batch algorithms is that they usually require heavy computations, and that they are not able to work in real time. They will only be able to work in real time if accurate predictions are computed, but accurate predictions can only be computed in combination with accurate dynamic models, which in principle is not compatible with an on-board orbit determination concept.
- The major advantage of the Kalman filters is their capability to work in real time, every time a measurement is received a new estimation of the state can be computed, The major drawback of these algorithms is their low robustness, as they are very sensitive to anomalous measurements or events. They require very often a fine tuning of the noise and information matrices. It would be difficult to fulfil the integrity requirements using a Kalman filter algorithm.

As it has been mentioned before, the proposed algorithm is a combination of the two described algorithms. Therefore it would be possible to combine the high robustness (integrity) and accuracy of the least squares batch algorithms, with the real time capabilities of the Kalman filters. The least square algorithm with a priori information is briefly described here.

If an estimate and the associated covariance matrix are known at a time t_j, and an additional observation or observation sequence is obtained at a time t_k, the estimate and the observation can be combined in a straight forward manner to obtain the new estimate $\hat{x}_k$.

The estimate $\hat{x}_j$ and P_j(covariance matrix) are propagated forward to t_k, using the following expressions:

$$\bar{x}_k = \Phi\left(t_k, t_j\right)\hat{x}_j$$
$$\bar{P}_k = \Phi\left(t_k, t_j\right)P_j\Phi^T\left(t_k, t_j\right)$$

Where $\Phi\left(t_k, t_j\right)$ represents the transition or propagation matrix. The problem to be considered can be stated as follows:

Given $\bar{x}_k, \bar{P}_k$ and some measurements ($y_k = H_k x_k + \varepsilon_k$), where the observation error is random with zero mean and specified covariance ($E\left[\varepsilon_k \varepsilon_j^T\right] = R_k \delta_{kj}$ and $E\left[\left(x_j - \hat{x}_j\right)\varepsilon_k^T\right] = 0$) find the best linear minimum variance unbiased estimate of x_k.

The solution to the problem can be obtained just by considering the a priori information as measurements. The problem can be solved using a normal least squares filter. Note that if $\hat{x}_j$ is unbiased, $\bar{x}_k$ will be unbiased since $E[\bar{x}_k] = \Phi(t_k, t_j)E[\hat{x}_j]$. Hence, $\bar{x}_k$ can be interpreted as an observation and the following relations will hold

$$y_k = H_k x_k + \varepsilon_k$$
$$\bar{x}_k = x_k + \eta_k$$

where

$$E[\varepsilon_k] = 0, \quad E[\varepsilon_k \varepsilon_j^T] = R_k, \quad E[\eta_k] = 0$$
$$E[\eta_k \varepsilon_k^T] = 0 \text{ and } E[\eta_k \eta_k^T] = \bar{P}_k$$

Now if the following definitions are used

$$y = \begin{bmatrix} y_k \\ .... \\ \bar{x}_k \end{bmatrix} \quad H = \begin{bmatrix} H_k \\ .... \\ I \end{bmatrix} \quad \varepsilon = \begin{bmatrix} \varepsilon_k \\ .... \\ \eta_k \end{bmatrix} \quad R = \begin{bmatrix} R_k & 0 \\ ... & ... \\ 0 & \bar{P}_k \end{bmatrix}$$

The observation equations can be expressed as $y_k = H_k x_k + \varepsilon_k$, and the weighted least squares solution can be applied to obtain the following estimate for $\hat{x}_j$.

$$\hat{x}_k = (H^T R^{-1} H)^{-1} H^T R^{-1} y$$

In view of the previous definitions:

$$\hat{x}_j = \left\{ \begin{bmatrix} H_k^T & : & I \end{bmatrix} \begin{bmatrix} R_k^{-1} & 0 \\ ... & ... \\ 0 & \bar{P}_k^{-1} \end{bmatrix} \begin{bmatrix} H_k \\ ... \\ I \end{bmatrix} \right\}^{-1} \left\{ \begin{bmatrix} H_k^T & : & I \end{bmatrix} \begin{bmatrix} R_k^{-1} & 0 \\ ... & ... \\ 0 & \bar{P}_k^{-1} \end{bmatrix} \begin{bmatrix} y_k \\ ... \\ \bar{x}_k \end{bmatrix} \right\}$$

or in expanded form,

$$\hat{x}_k = (H_k^T R_k^{-1} H_k + \bar{P}_k^{-1})^{-1} (H_k^T R_k^{-1} y_k + \bar{P}_k^{-1} \bar{x}_k)$$

The covariance associated with the new estimate is

$$P_k = E[(\hat{x}_k - x_k)(\hat{x}_k - x_k)^T] = (H_k^T R_k^{-1} H_k + \bar{P}_k^{-1})^{-1}$$

The following remarks are pertinent to the previous equations:

1. The vector y_k may be only a single observation or it may include an entire batch of observations.
2. The a priori estimate, $\bar{x}_k$, may represent the estimate based on a priori initial conditions or the estimate based on the reduction of a previous batch of data.

The approach proposed is then based on the processing of small batches of data (around a few minutes) but using the covariance matrix obtained in the previous batch estimation as additional observations for the current batch. The arc length of the process shall be adjusted (envisaged value 5 minutes) and the weight to be given to the measurements and the a priori information (covariance matrix) shall also be adjusted. Those parameters will be adjusted by considering the stringent integrity requirements. The real time capabilities are obtained thanks to the way the ephemeris to be sent to the user is computed. This message is computed by performing a fit, in a least squares sense, of the parameters of a simple orbit model to the latest estate estimates. The parameters of the model are sent to the user at regular time intervals. For a satellite flying at a geosynchronous altitude, those parameters will remain valid over a period not shorter than two hours.

To test the feasibility of this type of algorithms the precise orbit determination software BAHN (developed at ESA/ESOC) has been taken. The BAHN software is a batch least squares algorithm, and it has been converted into a reduce dynamic algorithm by performing some minor modifications. Those modifications are schematically represented in Figure 4 and Figure 4.

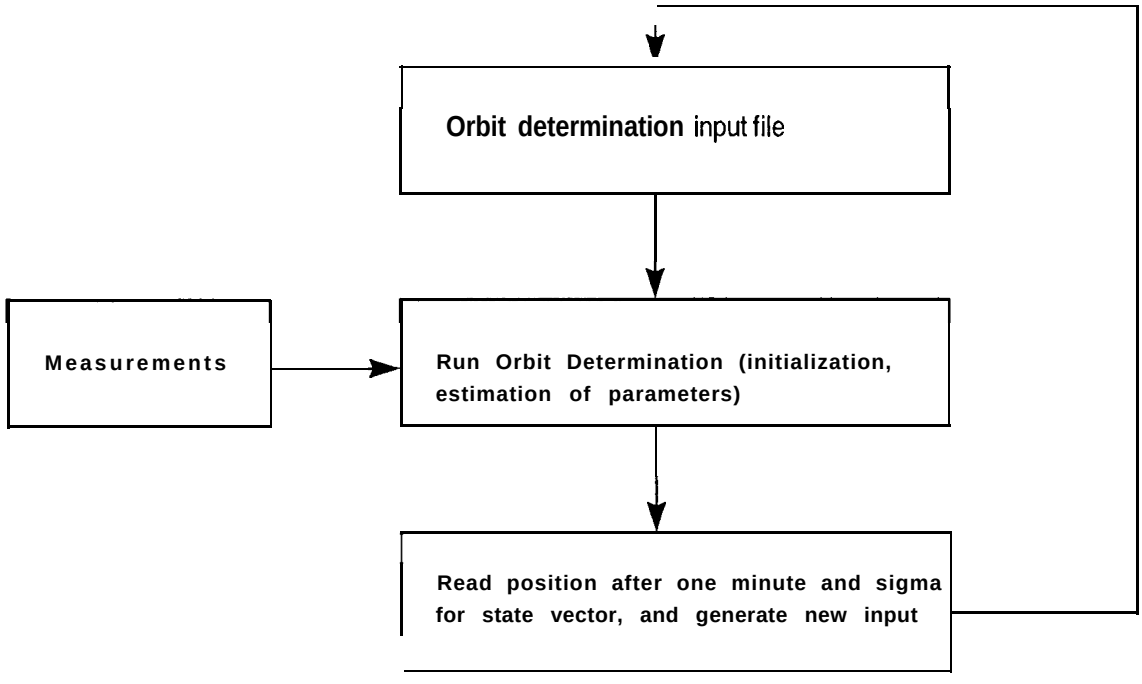

Figure 3 Schematic representation of the implemented algorithm

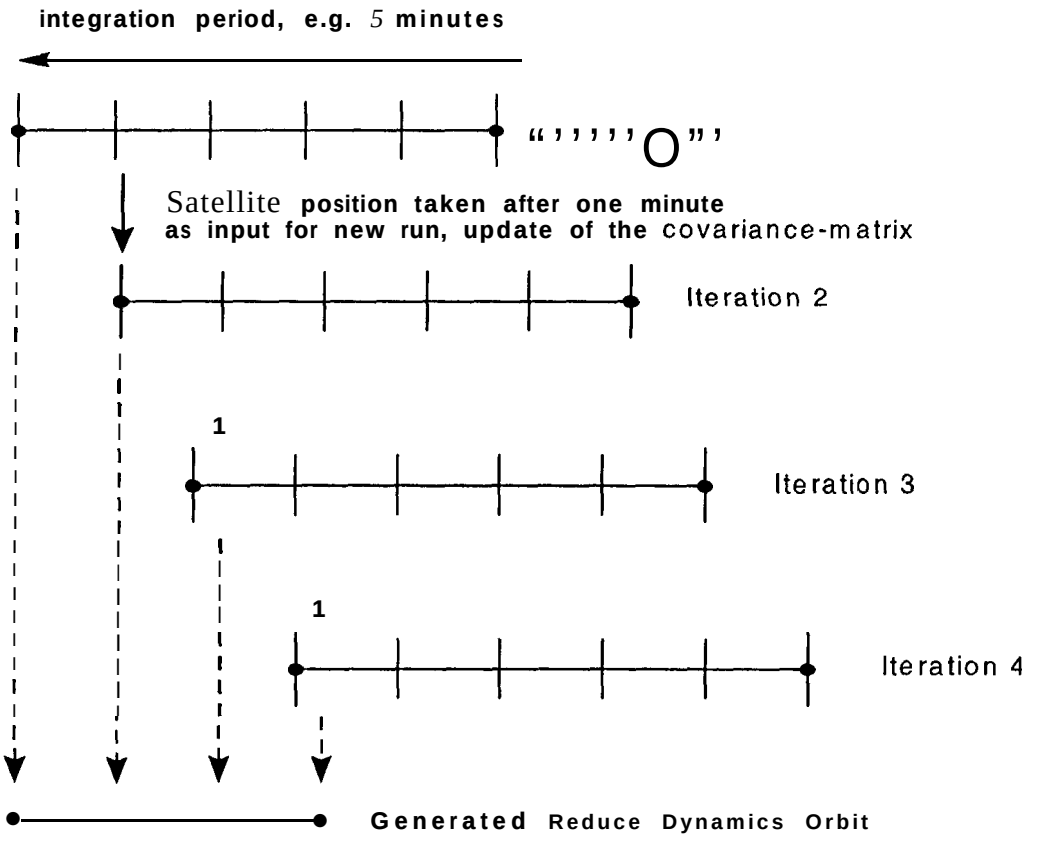

Figure 4 Schematic representation of the implemented algorithm

SIMULATION RESULTS

To test the performances of the implemented algorithms some simulations have been performed. The orbit selected has been an inclined geosynchronous orbit (IGSO) as future satellite navigation systems may be based on those orbits. The ground tracks described by an European GNSS constellation composed by satellites flying in GEO and IGSO orbits is represented in Figure 5.

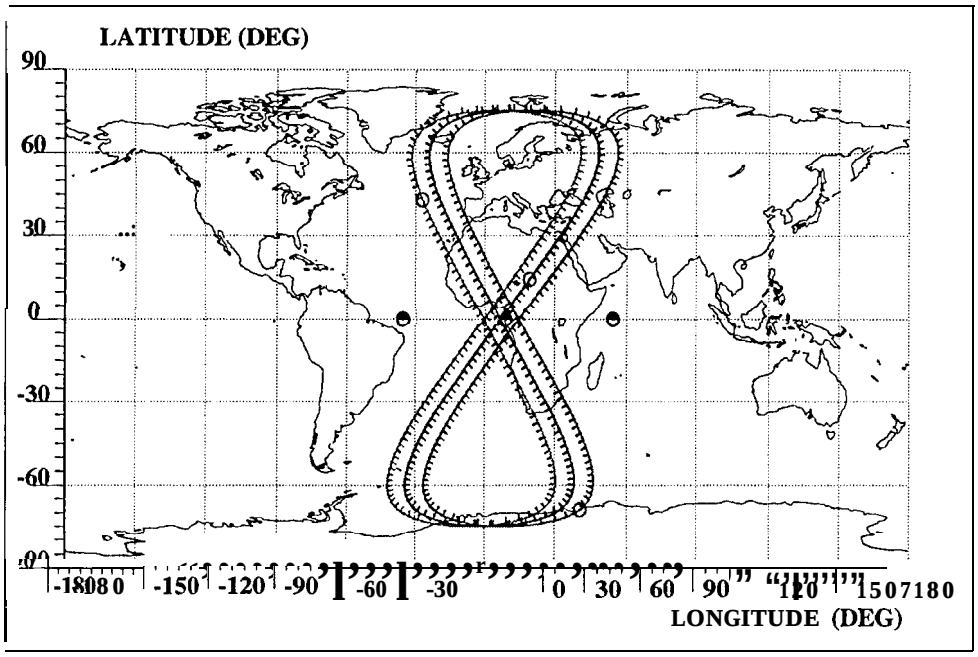

Figure 5 Ground track for the ENSS constellation

To simulate the tracking data realistic errors have been introduced in the models affecting the satellite motion, and the measurements. Simulations have been validated by using real data from GPS and GEO satellites, unfortunately it has not been possible to validate the measurement simulation process using real data from an IGSO satellite, as there are no satellites flying in those orbits.

Measurements (two way range) have been simulated with a measurement rate of 5 seconds. The dynamic models used for the measurements generation are represented in the table below, there also the models that have for been used for the orbit computation are represented.

Item	Generation of measurements	Short arc determination
Gravity field	JGM (9x9)	GEMT3 (2x0)
Solar perturbations	Used	Not Used
Lunar perturbations	Used	Not Used
Solid tide perturbations	Used	Not Used
Ocean tide perturbations	Schwiderski (6x6)	Not used
c.p.r. accelerations	Not used	Used

Table 1 Dynamic models considered

A total arc length of 4 hours was studied. Figure 6 shows this ground track of the satellite for that period.

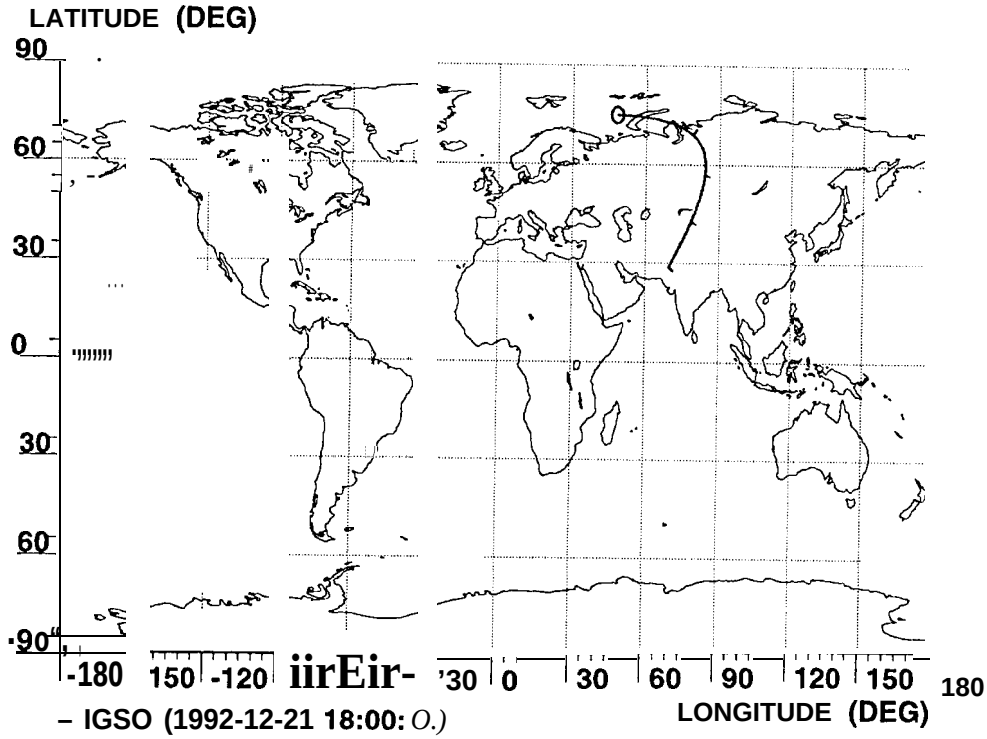

Figure 6: Part of the satellite arc from the IGSO used for the reduce dynamic orbit determination simulations

Three different tracking stations network were studied. First the case with only European tracking stations. Those consist of the following stations:

- Reykjavik
- Hammerfest
- Rome
- Aberdeen
- Stilly
- Ankara
- Munich
- Cádiz.

This network will be referred to as "European". A second case is the case with tracking stations divided more regular] y over the Earth's surface with respect to the satellite orbit. These stations are:

- Hammerfest
- Cádiz

- Ankara
- Usuda
- Djakarta
- Ceylon
- Alaska
- Malindi
- Irkutsk

This network will be referred to as “Well Distributed”, As a last case a network is used with good geometry but with only a very few tracking stations. This network consists of the following stations:

- Hammerfest
- Malindi
- Irkutsk
- Cádiz

This network will be referred to “Reduced Network”. All the stations used for the analysis here are depicted on the map in Figure 7.

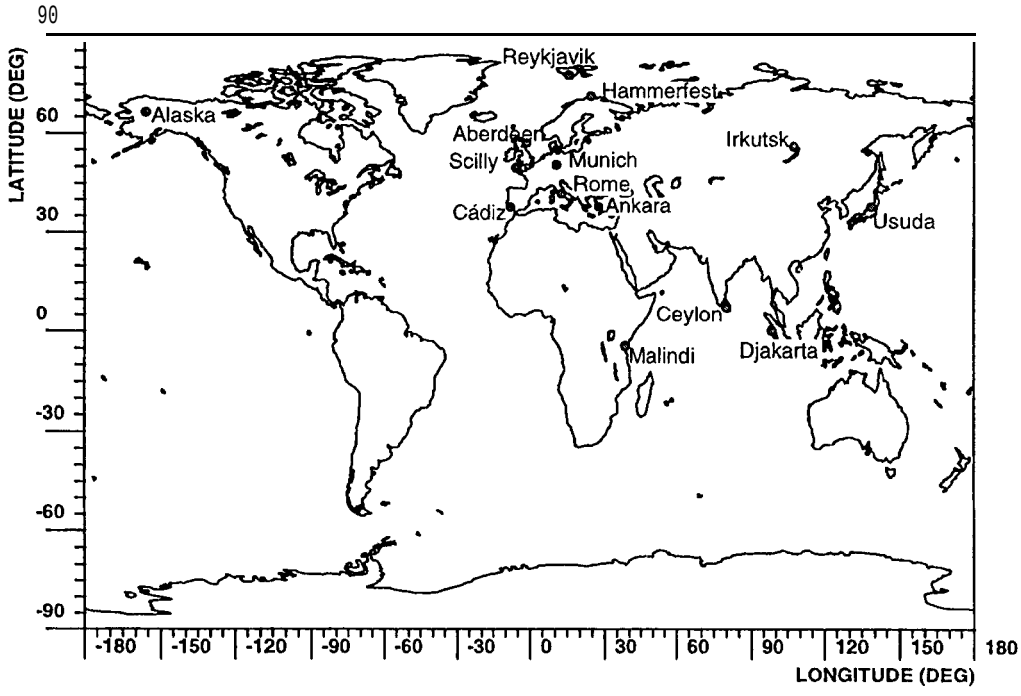

Figure 7: Tracking stations used for different case of reduce dynamic orbit determination

First from the generation of the simulated measurements a reference orbit was created. This orbit was used as the true orbit. Then with different set-ups for the tracking network, orbits were calculated using the reduce dynamic algorithm. The resulting orbits were compared with the reference orbit by means of the RMS of the differences in radial, along track and cross track direction. This was done for the three tracking station network for two different case.

. The first case is the nominal case optimal for the reduce dynamic algorithm, i.e., very good measurements are present for all stations. This means measurements have been generated with a noise of 10 cm and no station dependent biases are present.

. The second case is to see the effect of measurements with more noise and with biases. A noise of 1 meter was used and for all stations biases were generated with a sigma of 5 meters, This was only done for the European network and the emphasis here is more on the effects of the biases. One case will be studied in which the biases are estimated and in the other case the biases will not be estimated in the process

The following table depicts the results for the first case, with the three different tracking station network and good measurements (no biases and measurements with a sigma of 10 cm)

Tracking network	Radial (cm)	Along track (cm)	Cross track (cm)	Total RMS (cm)
European network	10.17	36.53	92.98	57.97
Well Distributed Network	2.50	17.39	11.59	12.15
Reduced Network	3.62	47.24	8.29	57.85

Table 2 Estimated accuracy of the computed orbits

These results show the power of the reduce dynamic algorithm in the presence of good measurements. All three cases give results well below a meter and in the case of the Well Distributed Network the differences are even on the decimetre level. The results for the Reduced Network are a little misleading because in the first part of the orbit determination the Malindi station is not tracking the satellite. When Malindi was within the visibility of the satellite it was observed that the results were comparable with that of the Well Distributed Network. Therefore the following conclusions can be made:

. Reduce dynamic orbit determination is **very powerful** if **accurate measurements are present** with a geometrically well distributed network of ground stations. Also only a few ground stations, but with **good geographical distribution** lead to good results.

For the second case, with measurements with 1 metre noise and station dependent biases the results are depicted in following table.

Tracking network	Radial (cm)	Along track (cm)	Cross track (cm)	Total RMS (cm)
European, biases estimated	1106.92	1731.63	8915.14	5282.16
European, biases fixed	60.58	1601.27	1182.96	1149.95

Table 3 Estimated accuracy of the computed orbits

These results indicate that the reduce dynamic algorithm looses its strength when no precise measurements are present. The case in which the station dependent biases were estimated showed no convergence and was only deteriorating in means of orbit differences.

The case in which the biases were not estimated shows better performance, but still in the order of meters. However, the difference here is that the orbit seemed to be converging. This can be seen in Figure 8.

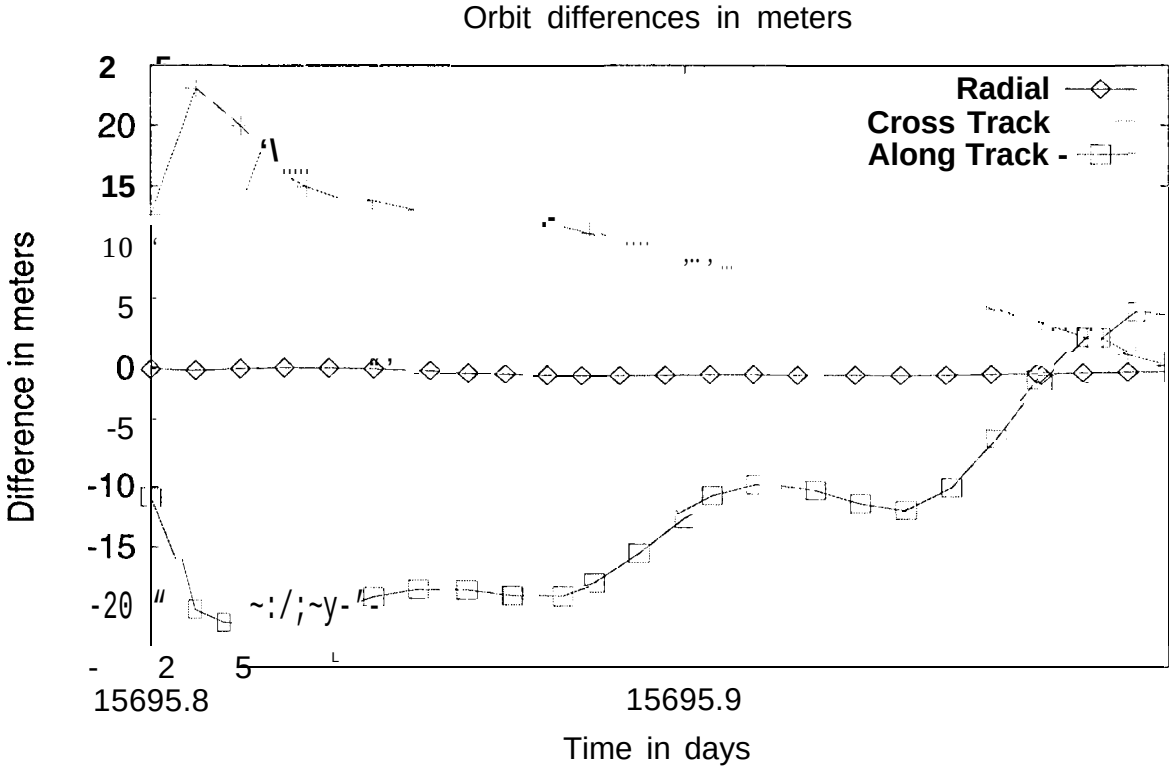

Figure 8: Plot of orbit differences in radial, along track and cross track direction for the reduce dynamics algorithm with a European network and the biases fixed

The time it takes to complete one iteration (in this case this correspond to five minutes of data) on a Sun Spare Ultra, is about 10 seconds. It has to be reminded here that this can even be faster if the orbit determination package is modified in a proper way so that it is not initializing all of its parameters each time it is run. It can be concluded therefore that the reduce dynamic algorithm can be successfully used for real time purposes. Moreover

it is believed that, with dedicated software development, it is even suited for on-board orbit determination, since the dynamic models used for the reduce dynamics are quite simple.

The capability of the reduce dynamic algorithms to compute accurate orbits during manoeuvre periods has been evaluated. Some orbital manoeuvres have been simulated and orbits have been computed using reduce dynamic algorithms. The major conclusion of this analysis is:

. The orbit determination accuracy to be achieved during manoeuvre periods is about the same as the obtained in periods without manoeuvres. Therefore the results presented in previous tables are also representative for manoeuvre periods. The orbit determination accuracy to be achieved is therefore not driven by the manoeuvre execution but for the tracking data quality.

CONCLUSIONS

The following conclusions have been derived from the analysis:

- A reduced dynamic algorithm has been derived from a state of the art dynamic algorithm. The reason for that has only been to tests the performances of the algorithm, but if an on-board implementation is required it would be better to start from a fairly simple orbit propagator, almost keplerian.

- It has been demonstrated that this type of algorithms will allow to accomplish the very stringent accuracy, integrity and continuity requirements for a future global navigation system.

- Results from preliminary simulations indicate that the describe algorithm is able to provide very accurate ephemeris if accurate measurements, from a well distributed network of ground stations, are available.

- This algorithm can be used for autonomous orbit determination, or to estimate orbits during critical periods, like manoeuvres.

ARP PROJECT: ABSOLUTE AND RELATIVE ORBITS USING GPS

Tomás J. Martin Mur
European Space Operations Centre, European Space Agency
D-64293 Darmstadt, Germany

Carlos García Martinez
GMV at ESOC

ABSTRACT

ESA's Automated Transfer Vehicle (ATV), a logistic and supply spacecraft for the International Space Station (ISS), will use GPS as the main positioning system for absolute and long range relative navigation. The ATV Rendez-vous Predevelopment (ARP) program is being carried out to increase European expertise on automated rendez-vous technologies. This program includes three Flight Demonstrations in which data from GPS receivers on-board two nearby spacecraft are collected, so they can be used to validate relative navigation algorithms using GPS, ESOC is participating in the project by computing absolute reference trajectories using precise GPS orbits and clocks. These trajectories are then compared with the results from the relative trajectory algorithm.

INTRODUCTION

GPS has been proposed as tracking or scientific instrument for several future ESA spacecraft. One of them will be the ATV, that will serve as a logistic and supply vehicle for the International Space Station. GPS is going to be used to determine the long and medium range relative position of the ATV with respect to the 1SS. For this GPS receivers and the associated antennas will be installed in both spacecraft. Before the concept can be used operationally, it is necessary to fine-tune it and validate it by using flight experiments with other spacecraft and ground simulations. The ATV Rendez-vous Predevelopment (ARP) program has the goal of validating methods for relative navigation, including relative GPS navigation. Within this program three Flight Demonstrations have taken place to collect GPS and other data from spacecraft performing rendez-vous. These data are then processed on-ground to test and validate on-board algorithms for relative navigation. Independent reference trajectories are

needed in order to use them as yardstick against which the results of the relative navigation algorithm can be compared.

ESOC was asked to calculate absolute trajectories using GPS as a relatively independent yardstick with respect to the relative trajectories that are computed using common-view differential observations.

THE ARP FLIGHT DEMONSTRATIONS

The three ARP Flight Demonstrations (FD) have already taken place. In all of them GPS receivers have been simultaneously operated in two spacecraft performing rendez-vous. The receivers used were SPS receivers modified to output raw measurement data. They produced C/A pseudorange, and L1 carrier and doppler and they had between 6 and 12 channels, The baseline for ATV is to use one-frequency receivers with a number of channels and antennas that should ensure a common visibility of at least four GPS satellites.

ARP FD- 1 took place between November 19 and December 4, 1996. It was performed during the STS-80 Shuttle flight and it involved the Shuttle acting as chaser spacecraft and the Orfeus-SPAS retrievable satellite acting as target. The Orfeus-SPAS was equipped with the 9-channel Laben ARP GPS receiver and the Shuttle had the 6-channel Trimble TANS Quadrex receiver. Data (GPS and GNC) were simultaneously collected during a free-flight period and during retrieval.

ARP FD-2 took place in May 1997 during Shuttle flight STS-84 to the MIR space station. For this flight the Laben ARP GPS receiver was installed on the Shuttle and the GPS data from MIR was obtained from the MOMSNAV receiver. This receiver has two blocks of 6-channels and each of them is connected to one antenna, one to a out-looking antenna in the Priroda module and the other to a side-looking antenna in the same module. Simultaneous data was collected only during separation.

ARP FD-3 took place in September/October 1997 during Shuttle flight STS-86 to the MIR space station. The configuration was the same as for FD2 and it seems that simultaneous data from both the docking and the un-docking will be available. The data from MIR had to be brought back to the ground on physical support by a later flight of the Shuttle (Soyuz for FD2).

POST-FLIGHT PROCESSING AT ESOC

ESOC processed the GPS data together with GNC data and IGS products [Martín Mur et al, 1997]. The GNC data is used to model the spacecraft attitude and the possible thruster firings, The IGS products that are used are ESOC'S final orbits and 30 second clocks. The approach that is used to determine the trajectories in the ARP context has to be different to that used for standard GPS POD because the data is collected over periods of only a few hours, the spacecraft involved may be performing attitude or orbit manoeuvres, the receivers are one

frequency SPS models and because the spacecraft altitude is so low, non-propulsive dynamics (specially drag) can not be modeled to a very high degree of accuracy.

The approach that we follow is to use pseudorange and phase observable corrected with the ESOC precise orbit and clock products for the GPS satellites. Spacecraft state parameters, including clock parameters, are obtained using a precise orbit propagator together with a Square Root Information Filter (SRIF). The propagator includes empirical accelerations, and the SRIF produces filtered and smoothed estimates of the parameters, including empirical accelerations, and the covariance.

So far the data for FD1 and FD2 have been processed and we expect to receive and process the data for FD3 in the next months.

CRITICAL ASPECTS FOR ARP TRAJECTORY ESTIMATION

The critical aspects for this work, as already identified in our preparatory activities Martín Mur et al, 1995], are the following:

- Receiver characterization and performance
- Dynamical modeling
- Ionospheric correction

Receiver characterization is important because three different receivers from three different manufactures are being used. These receivers do not output RINEX standard GPS observable because they do not produce simultaneous carrier and pseudorange measurements for all channels, the pseudorange is output in the form of ambiguous code phase and time tags do not follow the RINEX standard. Each receiver uses a different data format and the data has to be preprocessed to correct biases that sometimes are not well defined. The receivers were designed to provide SPS solutions, in this way their precision and accuracy are not as good as for geodetic receivers. As an example, the pseudorange specification for the Laben receiver was of 10 m error. This may be enough for stand alone SPS (considering that selective availability has 30 m rms error), but it is not good when the receivers are used in differential mode.

Dynamical modeling is a problem because the spacecraft are flying very low (400 km), they have large and changing drag and solar radiation pressure areas. Furthermore they may be performing orbit and attitude control thrusting that are only known to a level of about 3 mm/S^2 and have moving parts that change the centre of mass location in body fixed axes. This has made it necessary to implement the estimation of empirical acceleration in our filter.

The ionospheric perturbation on carrier and code can not be calculated from the measurements because only one frequency is available and the high pseudorange noise precludes the use of techniques as those discussed in [Martin Mur et al, 1995] like the code-carrier ionospheric free combination. Ionospheric corrections from ground based receivers are of no avail because the spacecraft are flying not below but through the ionosphere, even

close to the maximum. It was decided to use the integration of the IRI-95 electron density model [Bilitza 1990], despite the fact that it does not include the effect of the plasmasphere on the carrier phase advance or the code delay.

RESULTS FOR THE FIRST TWO FLIGHT DEMONSTRATIONS

For FD1 [Martin Mur, 1997] data were collected during two phases, a dynamically quiet phase in between deployment and retrieval and a dynamically noisy phase during retrieval including grappling of the Astrospas by the Shuttle Remote Manipulation System (RMS). Carrier phase could be fitted to the centimeter level and pseudorange to the five meter level. The accuracy of the trajectories that were obtained is estimated to be about 30 cm rms for the in-between phase and about 1 meter for the retrieval, with degraded performance during grappling.

For FD2 [Martín Mur, 1998] data were recorded only during the separation and in that phase the Shuttle made a number of attitude correction manoeuvres. Data from the side-looking antenna in MIR were of questionable quality and it seems that the behavior of the MOMSNAV receiver is not yet fully understood. Solutions have been obtained with residuals in the centimeter range for phase and in the 5 meter range for pseudorange and it is expected that the solution accuracy is in the 1 meter rms level.

CONCLUSION

We have demonstrated the capability of producing improved trajectories for spacecraft using one frequency GPS receivers and IGS products. It is important to realize that the limiting factor for this kind of trajectory estimation is not the accuracy of precise GPS products, but by the accuracy of the measurements. For precise relative navigation the best results would be obtained using receivers that have been designed for the purpose, i.e. that can produce simultaneous, low noise carrier phase and pseudorange measurements.

REFERENCES

Bilitza, D. (cd.) (1990), International Reference Ionosphere 1990, NSSDC 90-22, Greenbelt, Maryland, 1990.

Martin Mur, Tomás J., J. Dow, N. Bondarenco, S. Casotto, J. Feltens and C. García Martinez (1995), Use of GPS for Precise and Operational Orbit Determination at ESOC, Proceedings of the ION GPS-95, September, 1995.

Martín Mur, Tomás J., J. Dow, C. García Martinez (1997), Absolute and Relative Navigation of Spacecraft Using GPS: The ATV Rendez-vous Predevelopment Flight Demonstrations, Proceedings of the 12th International Symposium on Space Flight Dynamics, June, 1997.

Martin Mur, Tomás J. (1997), ESOC ARP-FD1 Trajectory Reconstitution Analysis, ESA/ESOC, September, 1997.

Martin Mur, Tomás J., C. Garcia Martínez (1998), ESOC ARP-FD2 Trajectory Reconstitution Analysis, ESA/ESOC, February, 1998.

Poster Summary Papers

IGS Related Activities at the Geodetic Survey Division of Natural Resources Canada

C. Huot, P. Tétreault, Y. Mireault., P. Heroux,
R. Ferland, D. Hutchison and J. Kouba

Summary

In 1997 NRCan started submission to IGS of predicted orbits and estimated tropospheric delays. In 1998 NRCan will also start contributing ionosphere products in the recently adopted IGS IONEX format. No major modifications were made to the NRCan estimation strategy since the 1997 IGS Workshop except for the addition of new stations and the correction of erroneous ocean loading coefficients.

Rapid and Predicted Orbits and Clock Products

NRCan continues to use JPL's GIPSY-OASIS II software for its GPS processing along with the strategy described in the IGS Annual Reports. A new station selection strategy based on using at least one out of *n* stations in various geographic sub-region of the IGS tracking network was implemented. The strategy ensures that a network with a strong geometry is available early enough in the day to allow sufficient time to process and submit to IGS the daily rapid solutions. The new strategy has resulted in a more consistent quality of the NRCan rapid products which currently have rms of about 10 cm for satellite positions and 0.5 ns for satellite clocks with respect to IGR products. Rapid Earth Orientation Parameters (EOP) solutions are also submitted. The better selection of stations also resulted in fewer failures to submit rapid solutions to IGS on time. However, for some regions within the IGS tracking network, it is still difficult to consistently retrieve data on time for the processing.

In addition to the rapid orbits and clocks NRCan also provides predicted orbits on a daily basis to IGS. A 2-day prediction is obtained from 4 IGR rapid orbit solutions by estimating 6 Keplerian elements and 9 radiation pressure parameters using the Bernese software version 3.5. The IGR *x* and y Pole position series are used along with the Bulletin A UT 1 series to provide the necessary Earth Orientation Parameters. The use of the Bulletin A UT1 series, initiated on GPS Week 934, has improved the z-rotation orientation of the NRCan predicted orbits as can be seen on Figure 1. An annual trend of about 10 cm in amplitude has been observed in the z-translation orientation of the NRCan predicted orbits (not shown here). NRCan predicted orbits **are** currently about 50 cm median RMS with respect to IGR orbits for non-eclipsing satellites and about 100 cm for eclipsing satellites.

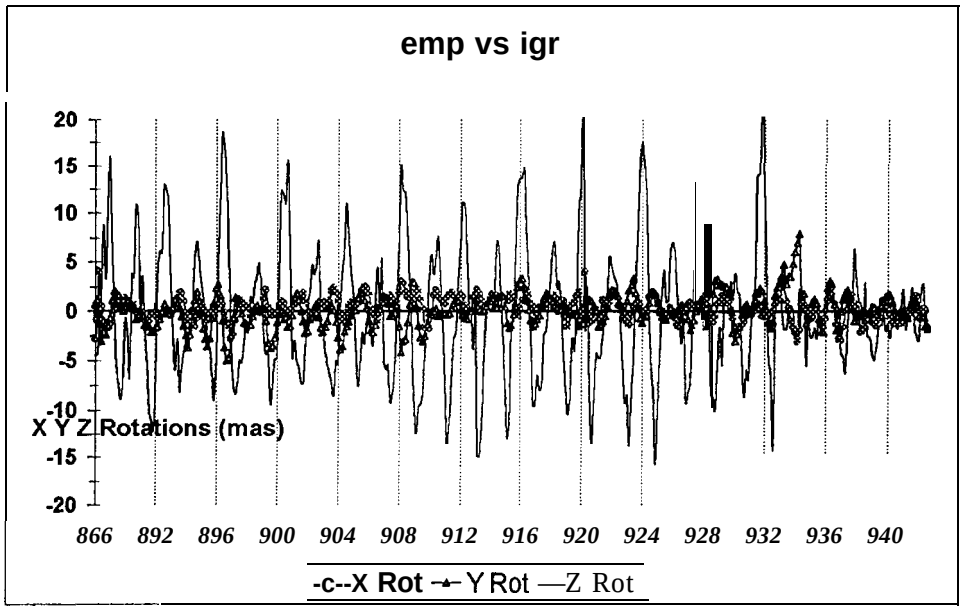

Figure 1. NRCan Predicted vs IGR orbits

Ionospheric Modeling

NRCan, **in** support of the Canadian Active Control System (CACS), has developed a regional grid model of ionospheric delays and is currently implementing **a** global solution in the IONEX format for future **submission to IGS. The** NRCan **ionospheric model is currently based on 10 to 15 regional stations covering the Canadian territory. It is computed using carrier phase smoothed pseudo-range observations with an elevation cut-off angle of 15 degrees and elevation dependent weighting. A spherical single layer shell at 350 km elevation and a cos z mapping** function **are used. The model has a 24 hour temporal resolution and uses a sun-fixed/geographic reference frame. Table** 1 **presents the precise point positioning monthly averaged daily rms which can be currently achieved with the single layer model and satellite differential code biases.**

Table 1. Point positioning using NRCan ionospheric modeling

Monthly Average of Daily RMS
Position Estimates at 15 min. intervals
Station NRC1, January 1998

RMS (m)			Processing Mode
Latitude	Longitude	Height	
1.3	0.7	3.6	L1
1.0	0.7	1.7	L1 + SLM
0.8	0.4	1.1	L1 + SLM + CAL
0.5	0.4	1.1	L3

L1 = L] Frequency
SLM = Single Layer Model
CAL = Satellite Differential Code Bias
L3 = Ionospheric Free Combination

Final Orbits, Clocks and Station Coordinate Products

A problem with NRCan ocean loading coefficients which resulted in a strong signal with a 13.7 day period in the NRCan 2.5 year station position residual series was corrected on February 23, 1997. A **recent spectral analysis of the NRCan station position residual series for GPS Weeks 894 to 938 confirmed that the erroneous ocean loading coefficients were indeed responsible for the artificial 13.7 day signal.**

Table 2 presents the weekly averaged differences between the NRCan and ITRF/IGS products computed for stations, orbits and EOP'S estimates. UTI-UTC was not included due to its long-term drift, which prevailed in the weekly averaged means and sigmas.

Table 2. Weekly Averaged Differences Between RNCan and ITRF/IGS Products For weeks 0836 to 0932.

Solution		Translation (cm)			Rotation (mas)			Scale(ppb)
		T]	T2	T3	R1	R2	R3	Sc
Stations	**(a)**	**0.0**	**-0.4**	**-0.2**	**-0.092**	**-0.017**	**-0.002**	**0.47**
sigmas		**0.1**	**0.2**	**0.1**	**0.044**	**0.025**	**0.016**	**0.33**
Orbits	**(b)**	**0.0**	**1.5**	**0.4**	**-0.352**	**0.072**	**-0.335**	**0.08**
sigmas		**0.8**	**0.9**	**0.6**	**0.145**	**0.129**	**0.285**	**0.09**
EOP (C)					-0.316	0.116		
sigmas					0.142	0.154		

(a) Combined NRCan weekly SINEX coord. solutions vs ITRF coord. for the 13 IGS fiducial stations.
(b) Weekly averaged transformations between NRCan and IGS daily orbits.
(c) Weekly averaged differences between NRCan and IGS daily polar motion.

ESA/ESOC IGS ANALYSIS CENTRE POSTER SUMMARY

Carlos García Martinez (GMv at ESOC), John Dow (ESA/ESOC),
Tomás Martfn Mur (ESA/ESOC), Joachim Feltens (EDS at ESOC),
Pelayo Bernedo (GMV at ESOC).

INTRODUCTION

The following are the main sheets of the poster that was presented in the workshop. It summarizes the current status and results of the ESOC IGS Analysis Centre.

ESOC ANALYSIS CENTRE: MAJOR CHANGES SINCE FEBRUARY 96

Date	Change
02/96	Estimation of small delta-v impulses every12 hours for the whole constellation to allow velocity discontinuity
11/02/96	ESA SINEX file available
30/06/96	New reference frame ITRF94. Subdaily polar motion according to Ray model. Antenna phase centre correction with the model IGS 01 .PCV. Estimation of EOP rates,
31/03/97	Estimation of sine and cosine radial one cycle per revolution empirical acceleration (instead of impulses every1 2 hours)
09/03/97	Saastamoinen tropospheric model replaced the Willman one
02/04/97	ESA predicted orbits available
21/04/97	Deadline of rapid orbits reduced from 23:00 to 21:00 UTC
22/07/97	Hatanaka compression implemented for the analysis and for the data distribution of the ESA receivers
30/1 1/97	Ocean loading implementation based on the Schemeck model

RAPID AND FINAL ORBITS

DIFFERENCES BETWEEN RAPID AND FINAL ORBITS

	FINAL	RAPID
PROCESSING STARTED	3 or 4 days after last collected data depending on data availability	at 14:00 UTC independent on data availability
PROCESSING TIME	12 hours	4 hours for 30 stations
ARC (hours)	12+24+12	12+ 24
NORMAL EQUATIONS FOR SINEX GENERATION ouTPuT	YES	NO

The orbit **modelling** is common. Per satellite we estimate the following parameters:
- Position and velocity at epoch.
- Scale for Rock 4T, y-bias, sine and cosine radial component one cycle per revolution empirical accelerations. These parameters replaced the delta-v impulses every 12 hours for all the satellites in March 1997.
- For **eclipsing satellites** the observations are excluded half an hour before and after the eclipse. Delta-v are estimated in the three orbital components at eclipse exit time.
-Any delta-v due to spacecraft **manoeuvres.**

PREDICTED ORBITS

Earth fixed positions taken from the rapid IGS solution are used as basic observable. The number of days for the fit is variable, currently set to four. If the IGR rapid orbit is not accessible our corresponding rapid solution plus cop's are used instead. Measurements of the last day have a weight three times the one of the initial days.

Per satellite are estimated **Rock 4T scale factor, ybias and sine and cosine one cycle per revolution empirical accelerations in the three orbital directions.** The initial state vector is taken from the corresponding rapid solution. It is also estimated.

Earth orientation parameters are taken from the rapid solution for the fit interval and from the IERS rapid service for the prediction. xp, yp and utl in the prediction interval are corrected **for the offset with respect to the IGS rapid eop's.**

Satellites are deweighted if
-they have been deweighted in the rapid solution
-are missing any of the days of the rapid combination
-are in eclipse period
-the orbit determination fit of the 4 igr orbits is poor.

Satellites with a extremely bad fit in the 4 day igr interval are replaced by the propagation of our last rapid solution. It has been proven that a propagation of a smaller arc gives better results.

ESTIMATION OF MANOEUVRES

Manoeuvres must be previously announced in the NANU'S and at least two receivers must track the manoeuvring satellite to detect the firing time. Two methods have been developed:

- Study of residuals of the phase triple differences. The time is determined by looking for a step in the triple differences. The preliminary delta-v value is estimated by energy change.

- Use of carrier phase time differences, An algorithm has been developed to detect delta-v changes based on the comparison of the observations to a propagated orbit.

Our orbit determination program BAHN estimates the impulse in three directions.

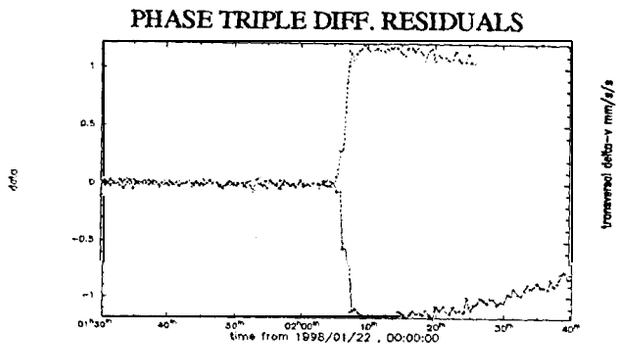

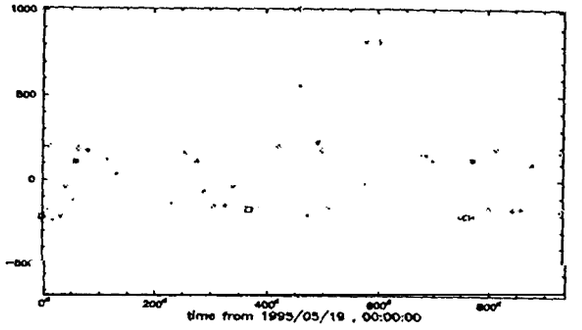

EARTH ORIENTATION PARAMETERS

Below are shown the differences of our estimations respect to the Bulletin B. Severa' improvements have been registered in the last two years, mainly due to the adoption of the Ray subdiurnal model in June 1996 and the estimation of one cycle per revolution empirical accelerations since March 1997.

The change to ITRF94 produced the discontinuities that can be seen in the pole comparison plot. The offset for our solution was about 0.82 mas in xp and 1.73 in yp.

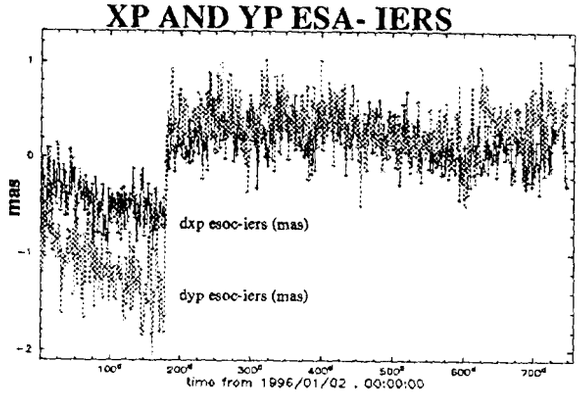

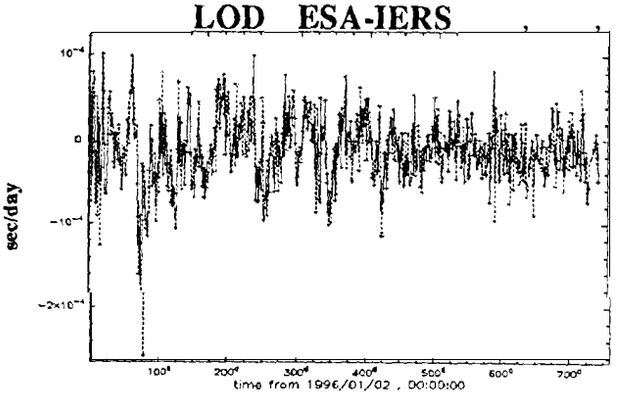

STATION COORDINATES

The stability of the station coordinates has been improved, especially in the vertical component, with the implementation of the **Saastamoinen** tropospheric model in March 1997 and also with the consideration of ocean loading based on the **Scherneck** model. That can be clearly seen below on the height estimation of **Maspalomas,** a station very much affected by the ocean loading effect. Several tidal effects, specially the fortnightly one, have been substantially reduced.

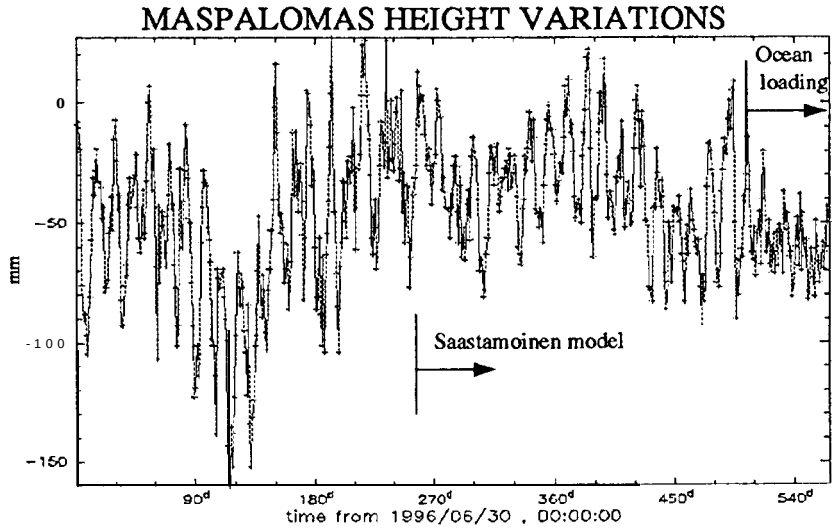

TRANSFORMATIONS FROM ESA SINEX TO ITRF

In this plots therms is presented for a time span of about two years. The ESA rms, scale factor and dy have converged to the igs solution since the introduction of the Saastamoinen model in March 1997.

The first 60 days of the plot the reference is **ITRF93** and it was changed to **ITRF94** on June 1996.

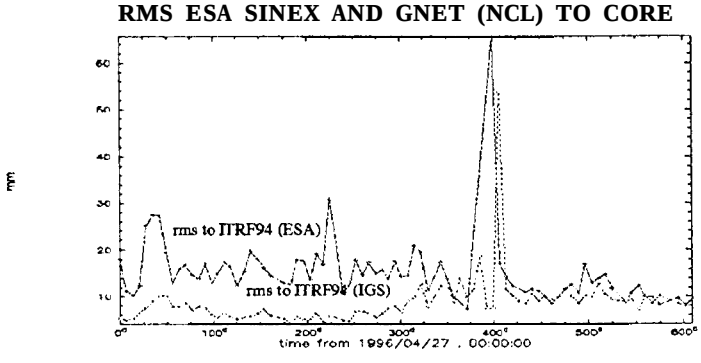

TROPOSPHERIC ESTIMATES

Tropospheric zenith path delays are produced in our routine analysis. They are estimated along with orbits, cop's and station coordinates. We use the **Saastamoinen** model since March 1997. The model consists of two hourly step functions with apriori values taken from the previous day.

In the following examples the results for three stations, USUD, TSKB and **TAEJ** from the same region are presented. The three curves show the same seasonal variation. Taejon and **Tsukuba** are located close to the sea level while **Usuda** is at about 1500 meters height. That explains the difference of about 400 mm between the curves. The geographical proximity between **Usuda** and **Tsukuba** makes both profiles to look very similar in spite of the height difference.

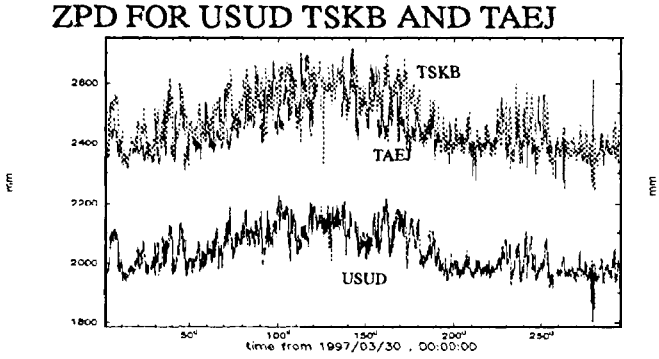

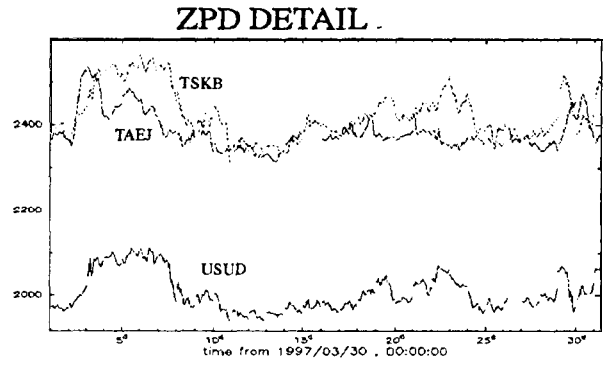

CONCLUSIONS AND OUTLOOK

- Since the beginning of 1997 we have incremented our IGS contribution with the production of predicted orbits.

-Rapid and final orbit solutions have improved through the estimation of empirical cyclic accelerations.

- Our products, especially station coordinates and atmospheric products, have been very positively affected by the implementation of the Saastamoinen tropospheric **model** and the **ocean loading,**

- The routine computation of ionospheric products has been recently started.

- Tests will be carried out to try to improve the dynamical model of the satellites, especially the eclipsing ones. This can have a positive impact in the predictions and rapid orbits when the visibility is poor. The arc lengths will be reviewed.

- **Glonass** data processing capabilities will be implemented in time for IGEX'98.

- We are currently using our orbits and clocks for the Automated Transfer Vehicle /Automatic Rendezvous Pre-development **(A TV/A TV) project, to demonstrate the capability to perform automated rendezvous operations using GPS.**

RECENT IGS ANALYSIS CENTER ACTIVITIES AT JPL

**David C. Jefferson, Yoaz E. Bar-Sever, Michael B. Heflin,
Michael M. Watkins, Frank H. Webb, James F. Zumberge
Jet Propulsion Laboratory, California Institute of Technology
Pasadena, CA 91109 USA**

SUMMARY

JPL activities as an IGS Analysis Center continued; regular deliveries of rapid (1 -day), and precise GPS orbits and clocks, Earth orientation parameters, and free-network ground station coordinates (now in SINEX 1.0) were maintained. Daily troposphere estimates in the IGS exchange format are now available. The estimation of site-specific tropospheric gradients have further improved the accuracy of our solutions. In 1998, a larger subset of the newly-augmented group of 47 IGS fiducial stations was put in use, and all freed-network solutions are made to align with ITRF96. Enhancements have been made to our site selection and automation processes. A timeline of our analysis strategy is shown in Table 1.

Table 1. Analysis evolution since 1997.

Action	Date
Produce troposphere files in IGS Exchange format	Jan 26, 1997
Produce station coordinate files in with SINEX 1.0 format	Jan 26
Produce free-network transformation files routinely	Apr 15
Do not process satellites not found on rapid-service orbit	Apr 23
Estimate tropospheric gradients	Aug 24
Use TurboRogue MAD2 (in place of MADR) as a fiducial site	Nov 9
Correct mismodeling of SRP for PRN03	Nov 9
Use NRC1 (instead of ALGO) as default reference clock	Dec 14
Use 32 hour nominal orbit interval, map final orbits for 30 hours	Feb 1, 1998
Use ITRF96 coordinates and velocities for 22+ subset of 47 IGS fiducials	Mar 1
Use free-network estimates in troposphere products	Mar 15

MAJOR NEW STRATEGIES AND PRODUCTS

Troposphere Solutions

Beginning with GPS week 890. JPL contributes solutions to the IGS troposphere estimate combination. These files contain our daily estimates of the total (wet + dry) zenith tropospheric delay at each site used in the global solution. Troposphere parameters are estimated using a satellite elevation cutoff of 15 degrees. The format of the troposphere products was designed by Yoaz Bar-

Sever (JPL) and Gerd Gendt (GFZ). Starting with GPS week 920, tropospheric gradients were added to the list of parameters estimated for each ground station. In implementing this strategy, the following modifications were made to the initial estimation process:

- The two gradient parameters are modeled as random walk with a sigma of 0.03 cm/sqrt(hour) and are estimated every five minutes.
- The Niell troposphere mapping function has replaced the Lanyi mapping function.
- The random walk sigma on the estimated zenith wet delay has been reduced from 1.02 cm/sqrt(hour) to 0.30 cm/sqrt(hour).
- The carrier phase post-fit residual rejection criterion has been reduced from 5.0 cm to 2.5 cm.
- Beginning week 949, troposphere products are representative of the free-network estimates (freed-network prior to this).

The JPL solutions are archived as
ftp://sideshow.jpl.nasa.gov/pub/jpligsac/<wwww>/jpl<wwww><d>.tro.Z.

Reference Frame

Beginning week 947, orbits, Earth orientation, SINEX station coordinates, and daily transformation files align with the ITRF96 reference frame. Nominal monument coordinates and velocities are taken from ftp://igscb.jpl.nasa.gov/igscb/station/coord/ITRF96_IGS_RS47.SNX.Z, and antenna heights from ftp://igscb.jpl.nasa.gov/igscb/station/general/igs.snx. As we use only 37 stations in our daily processing, we select a subset of the 47 sites designated by the IGS as fiducials in the following manner:

- Automatically include and constrain the following 22 sites when available ALGO DAV1 FAIR FORT GOL2 HARK IRKT KERG IUT3 KOKB KWJ1 MAC1 MAD2 MALI OHIG ONSA SANT TID2 TSKB WTZR YAR1 YELL.
- Allow the remaining 15 sites to be selected normally, based on geographic distribution. Constrain any of these that are IGS fiducials to their ITRF96 values.

The north-east-vertical transformation agreement between our 7-year ITRF94 solution and ITRF96 is 2, 2, and 11 mm for positions, and 1, 2, and 7 mm/yr for velocities.

RESULTS

One metric of performance is day-to-day orbit consistency. Figure 1 is a plot of JPL orbit repeatability (3drms) since 1995. Each data point indicates the median over all satellites and days for a particular GPS week. The daily number for a given satellite indicates the degree to which the precise orbit agrees with those of adjacent days near the midnight boundary. Weeks during which AS was off are marked with an 'X'. Contributing factors to the improving trend are the continuing expansion of the global network, the use of global phase ambiguity resolution, and the estimation of tropospheric gradients.

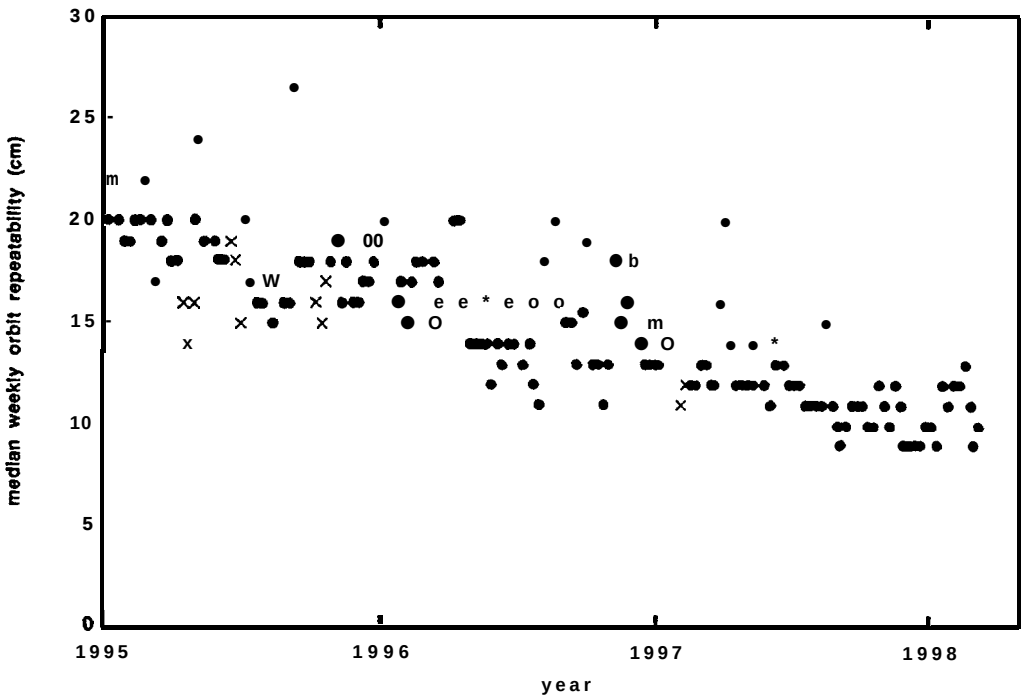

Fig. 1. JPL orbit repeatability (3drms) since 1995.

Ackno ***wledgement*** *The* **work described in this paper was carried out by the Jet Propulsion Laboratory, California Institute of Technology, under contract with the National Aeronautics and Space Administration.**

REFERENCES

Bar-Sever, Y. E., P. M. Kroger and J. A. Borjesson, Estimating Horizontal Gradients of Tropospheric Path Delay with a Single GPS Receiver. (Submitted for publication. Copies available upon request.)

Jefferson, D. C., M. B. Heflin, M. M. Watkins, F. H. Webb, J. F. Zumberge, Jet Propulsion Laboratory IGS Analysis Center Report, 1996, in *IGS* 1996 *Annual Report,* J. F. Zumberge, D. E. Fulton, R. E. Neilan, editors, IGS Central Bureau, Jet Propulsion Laboratory, Pasadena, CA, 1997

A REVIEW OF GPS RELATED ACTIVITIES AT THE NATIONAL GEODETIC SURVEY

Mark Schenewerk, Steve Mussman, Gerry Mader and Everett Dutton
National Geodetic Survey, NOAA
Silver Spring, MD 20910 USA

INTRODUCTION

The following, originally presented in poster format, is a brief summary of activities at the National Geodetic Survey (NGS) related to or of interest to the International GPS Survey for Geodynamics (IGS). First, a brief summary of orbit production and the quality of those products is given. This is followed by a description of a new effort to estimate total electron content (TEC) over the United States using the IGS and Continuously Operating Reference Station (CORS) network. These estimates are summarized in the form of TEC maps which are made available via the World Wide Web (WWW).

A SUMMARY OF ORBIT PRODUCTION AT NGS FOR 1997

- GPS ephemerides are made using the daily, 24 hour Receiver Independent EXchange (RINEX) data files processed with the page4 program.
- The observable is double-differenced, ionosphere-free phase with a data interval of 30 seconds and 15 degree observation elevation cutoff.
- The data are automatically edited with manual verification of the auto-editing.
- For the rapid products, initial conditions (position, velocity, two radiation pressure scale factors) are taken from the last epoch of the previous day's ephemeris. For the final products, the rapid is the source for the a priori orbital values.
- The National Earth Orientation Service, NEOS, Bulletin A (SERIES 7) e-mailings are used for a priori pole information. This series is updated for the Sunday production and kept for an entire week.
- The coordinates of the sanctioned sites are held constrained at the level of the sigmas distributed with the coordinates (Kouba, 1996). Two additional sites: MATE and MDO1 are also constrained. For the rapid products, additional sites may be constrained if significant data outages occur.
- The Cartwright and Taylor (1971 and Cartwright and Edden, 1973) solid Earth tidal potential, complete through degree three but including the newest Shida and Love numbers was used to removed the solid earth tide but no model for atmospheric or ocean-loading was applied.
- No ocean or atmospheric loading corrections are made.
- The standard antenna phase patterns were used (Rothacher and Mader, 1996).
- The hydrostatic (dry) component of the atmosphere was modelled and removed using Saastamoinen (1972) zenith delay and NMF mapping functions (Neill,

1996), A seasonal model for the surface temperature, pressure and relative humidity was used at all sites. Two hour wet tropospheric delays are estimated for all sites.

- Phase biases are estimated. No phase biases were fixed to their integer values.
- No operational changes have been made since January 12, 1997. The only software change occurred on June 30, 1997 when the automatic editor was upgraded.

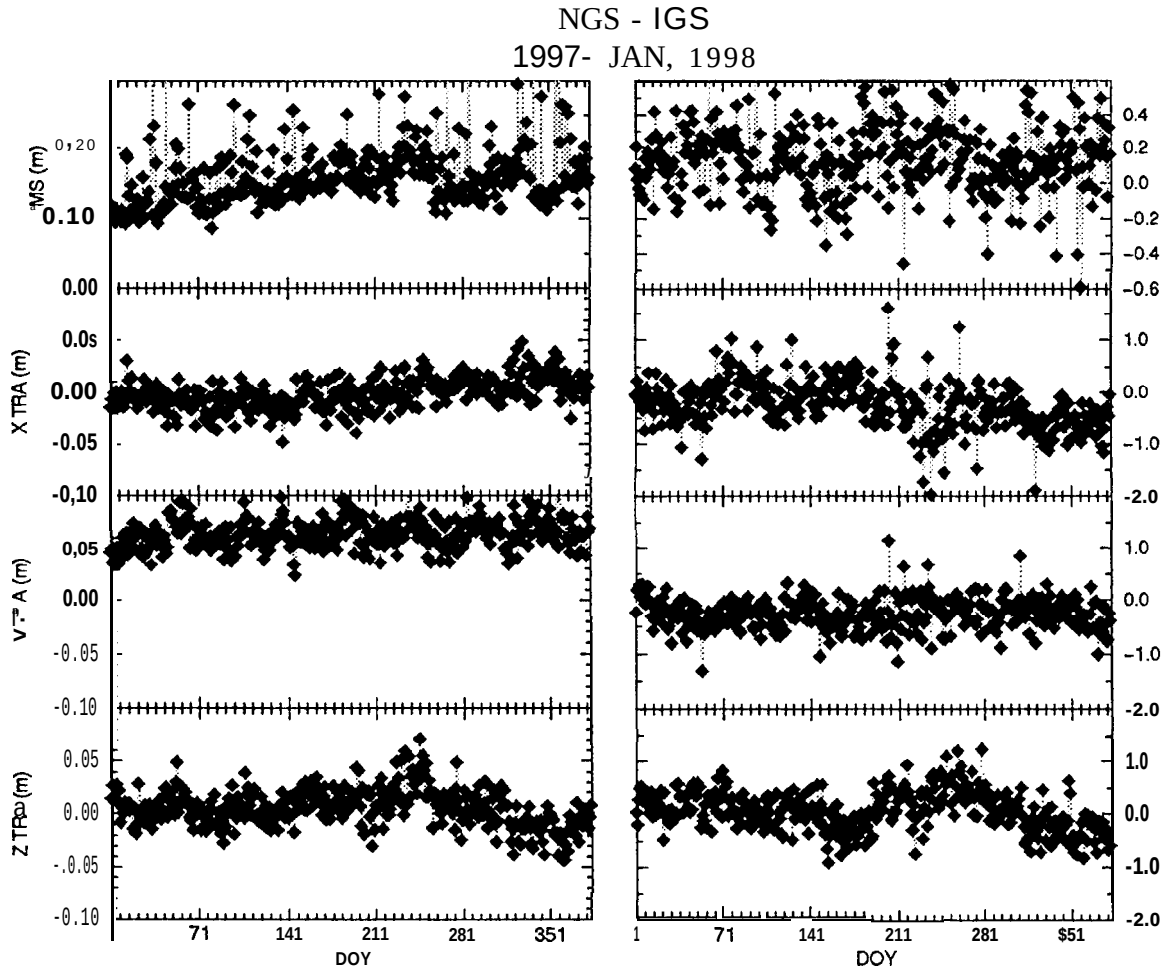

Figure 1 Comparison of the NGS product to the IGS Final. The panels show the RMS of fit, and the seven parameters of the transformation which yields the best fit. TRA = translation; ROT = rotation

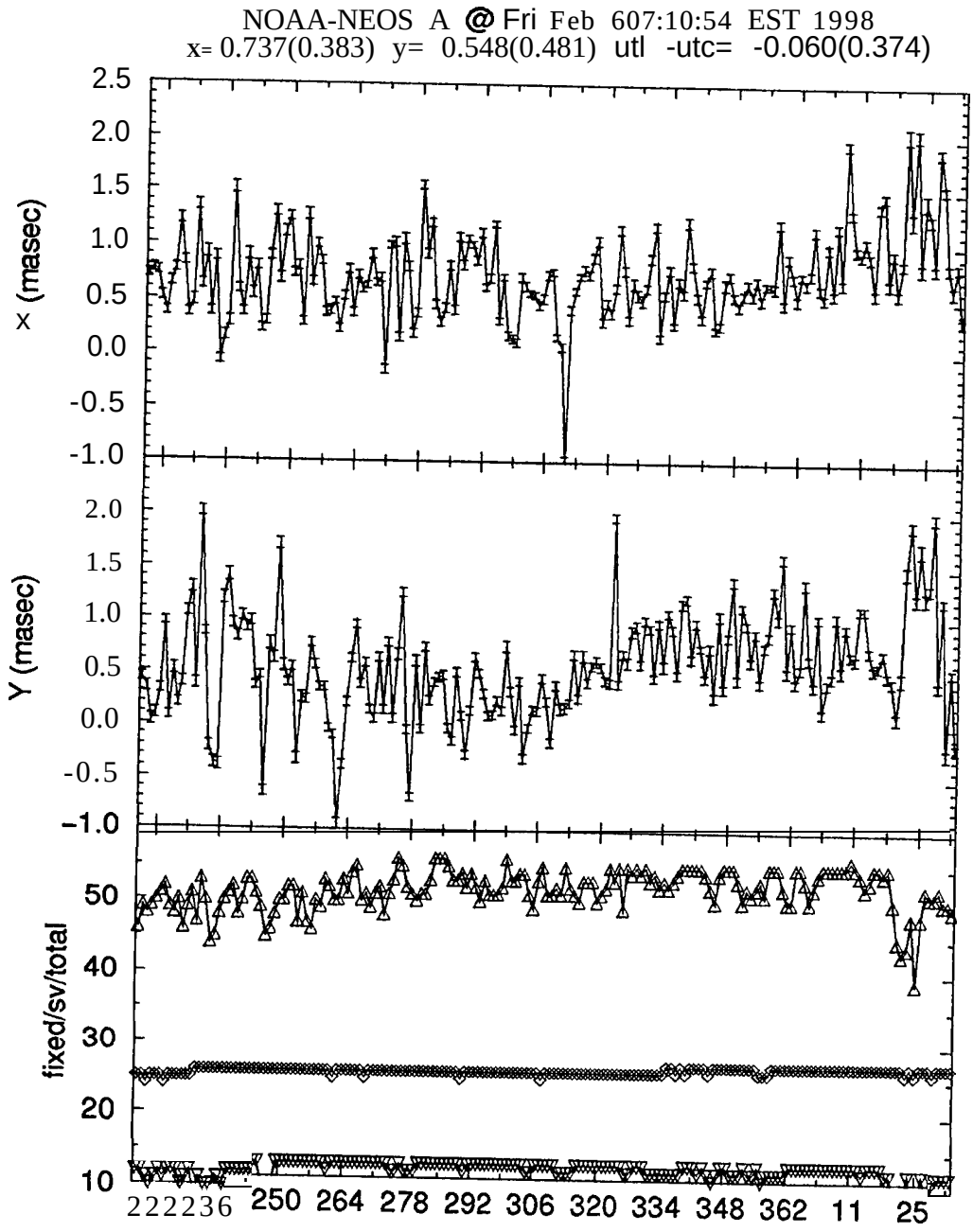

Figure 2 Comparison of the NGS X and Y Earth orientation parameters to the NEOS Bulletin A. The bottom panel shows the number of constrained, i.e. fixed sites (inverted triangles), satellites (diamonds), and total number of sites in each solution (triangles),

TOTAL ELECTRON CHANGES IN THE IONOSPHERE DURING IONOSPHERIC STORMS AS MEASURED BY THE CORS NETWORK OF GPS RECEIVERS

At each station of the CORS network, local models of TEC were constructed from carrier phase. These are displayed in the form of maps. Geomagnetic storms on 10 January, 15 May and 10 October, 1997 were studied in detail and are presented here. The TEC changes associated with the three event shown here depend strongly on latitutde. Maps are plotted of the daily maximum TEC minus the maximum of the average for several nearby days. This is a measure of the strength of the event which is independent of local time.

Developmental movies of the ionospheric maps for selected days are available at
http://www.grdl.noaa.gov/GRD/GPS/Projects/TEC

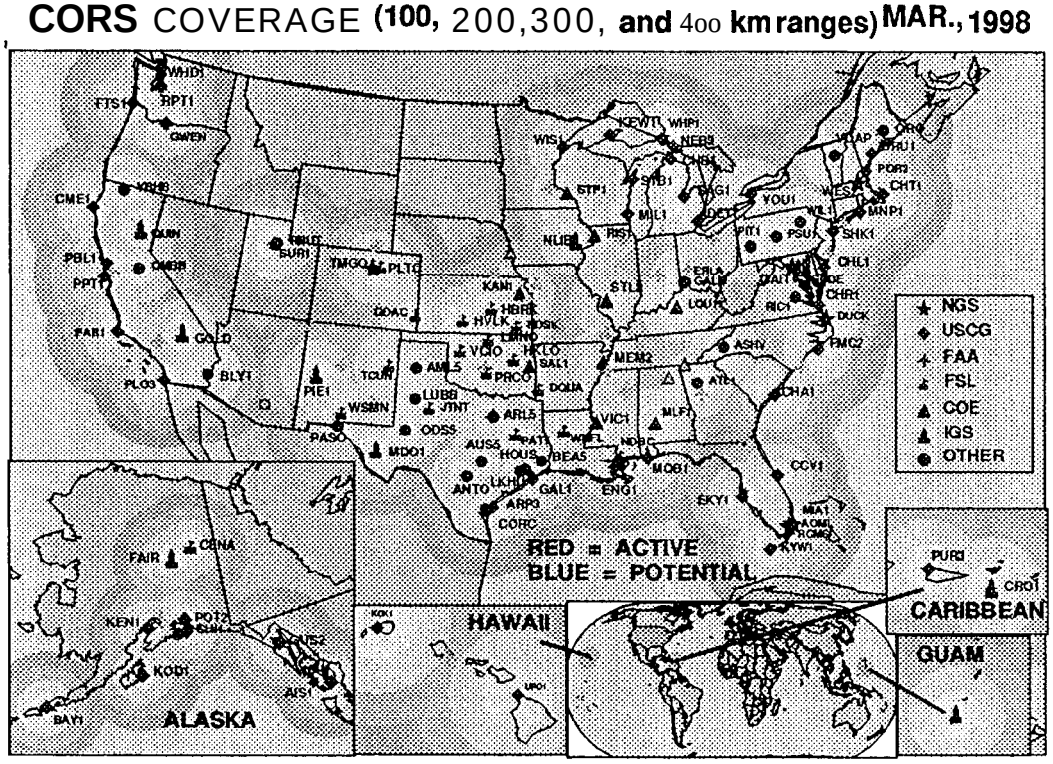

Figure 3 The CORS network as of March, 1998. Note that several IGS tracking sites are redistributed through the CORS data center.

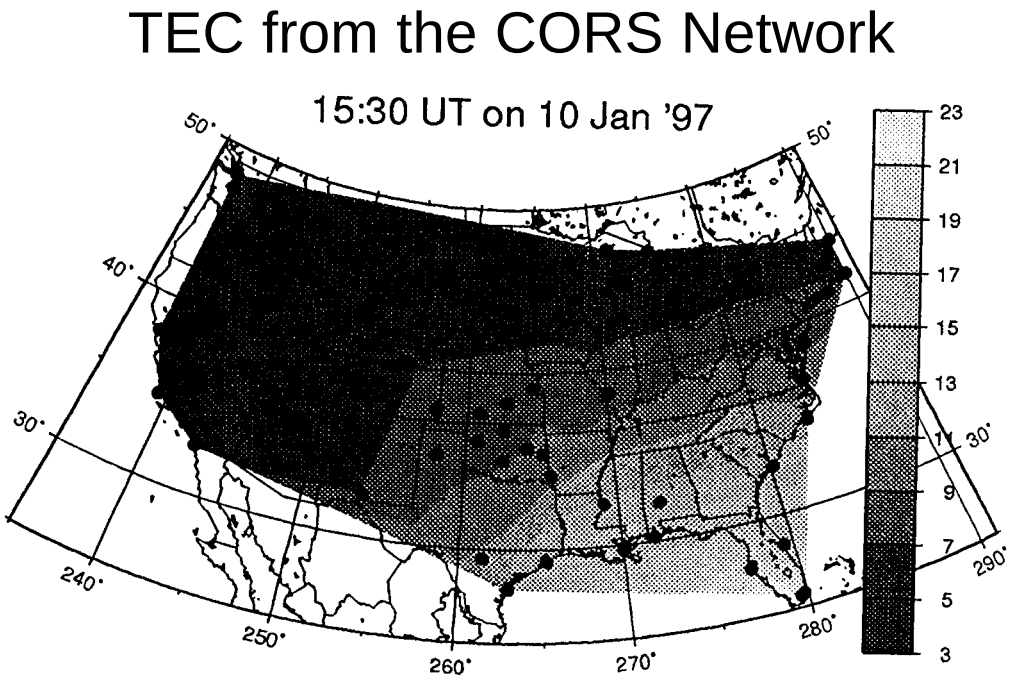

Figure 4 TEC map for 15:30 UTC on January 10, 1997

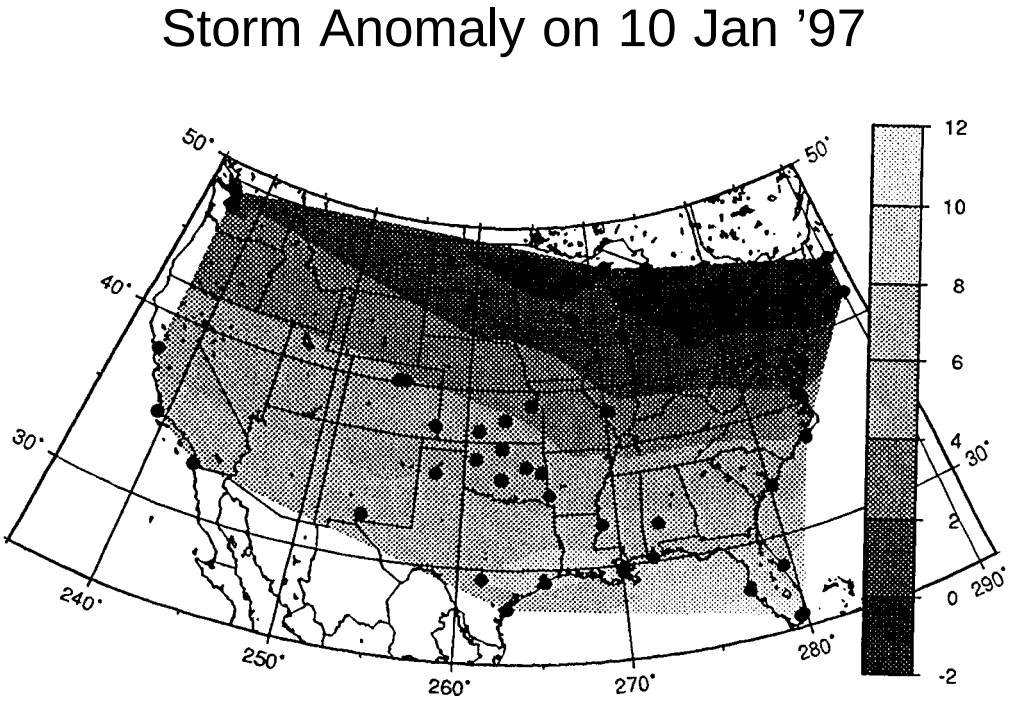

Figure 5 TEC maximum for January 10, 1997 minus the typical, average maximum for this period.

Storm Anomaly on 15 May '97

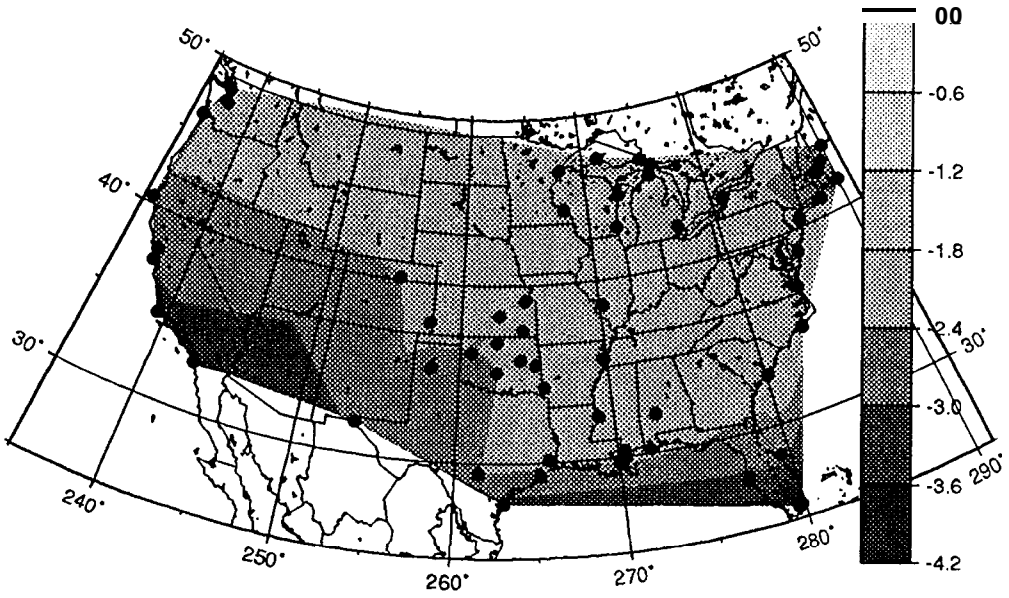

Figure 6 TEC maximum for May **15, 1997** minus the typical, average maximum for this period.

Storm Anomaly on 10 Ott **'97**

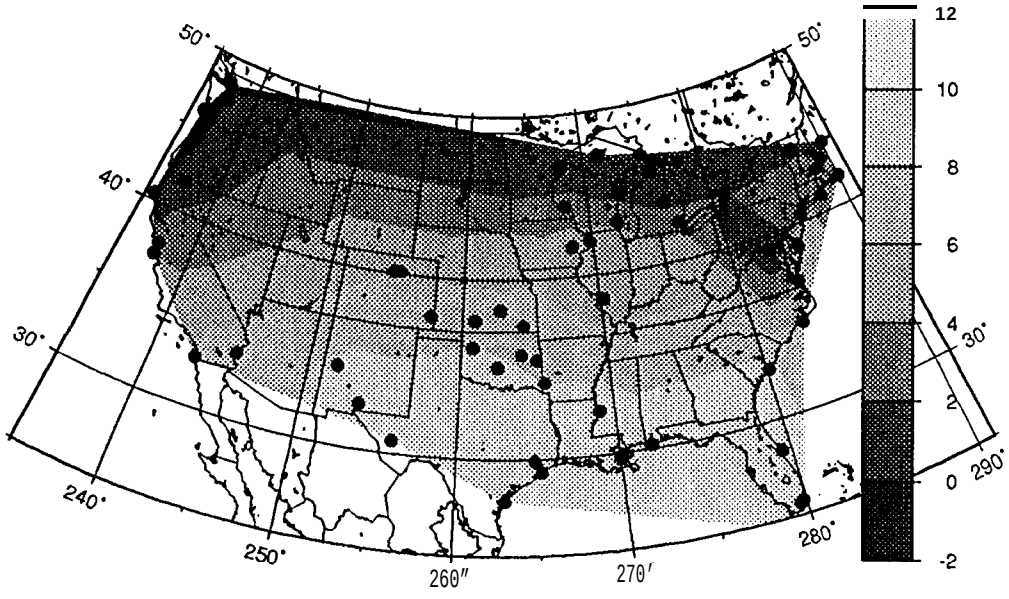

Figure 7 TEC maximum for October 10, 1997 minus the typical average maximum for this period.

REFERENCES

Cartwright, D.E., and R.J. Taylor, New computations of the tide-generating potential, *Geophys. J.R. astr. Soc.*, **23**, 45-74, 1971.

CartWright, D. E., and A.C. Edden, Corrected tables of tidal harmonics, ibid, 33, 253-264, 1973,

Kouba, J., Personal communication via email with subject "Comments on ITRF94 (fwd)", June 11, 1996.

Rothacher, M. and Mader, G.L., Personal communication via email with subject "Antenna Phase Center Corrections IGS_01", June 30, 1996.

Niell, A.E., Global mapping functions for the atmosphere delay at radio wavelengths, *J. Geophys. Res.*, **101(B2), 3227-3246, 1996.**

Saastamoinen, **J., Atmospheric correction for the troposphere and stratosphere in radio ranging of satellites, in The Use of Artificial Satellites for Geodesy,** *Geophys. Monogr. Ser. 15* (S.W. Henriksen et al., eds.), AGU, Washington, D. C., 247-251, 1972.

U.S. NAVAL OBSERVATORY: CENTER FOR RAPID SERVICE AND PREDICTIONS

J.R. Ray, J.R. Rohde, P. Kammeyer, and B.J. Luzum
Earth Orientation Dept., U.S. Naval Observatory
Washington, DC 20392 USA

INTRODUCTION

The mission of the U.S. Naval Observatory (USNO) includes determining the positions and motions of the Earth, Sun, Moon, planets, stars and other celestial objects, providing precise time, measuring the Earth's rotation, and maintaining the master clock for the U.S. The Earth Orientation (EO) Department contributes to this mission by collecting suitable observations and performing data analyses to determine and predict the orientation of the terrestrial reference frame within the celestial reference frame. The key parameters determined and disseminated are polar motion coordinates, universal time (UT1), precession, and nutation. The user community includes the U.S. Department of Defense, other U.S. government agencies, scientific researchers, and the general public. The primary applications are for high-accuracy navigation and positioning with an emphasis on real-time uses.

In order to accomplish these objectives, USNO collaborates closely with a large number of other groups and organizations. In particular, the U.S. National Earth Orientation Service (NEOS) is a partnership with the National Aeronautics and Space Administration (NASA) and the National Oceanic and Atmospheric Administration (NOAA) primarily to organize joint VLBI (very long baseline interferometry) operations to monitor Earth orientation. NEOS serves as the VLBI coordinating center for the International Earth Rotation Service (IERS). USNO and NEOS have an enduring commitment to VLBI in order to maintain accurate knowledge of UT1, the celestial pole, and the celestial reference frame, which is realized by the positions of about 600 extragalactic radio sources. This responsibility is shared with several non-U.S. agencies which contribute essential observing time on their VLBI telescopes.

As with VLBI, the capabilities of GPS also serve important USNO mission objectives. For that reason we have participated actively with the IGS since its inception. Recently, the US NO role in the IGS has grown and further expansion is expected. This report summarizes the current status and future prospects for US NO involvement with GPS and the IGS, together with some recent results.

IERS SUB-BUREAU FOR RAPID SERVICE AND PREDICTION

NEOS serves as the IERS Sub-bureau for Rapid Service and Prediction of Earth orientation parameters (EOPs). This function is carried out by the EO Dept. at USNO. EOP results contributed by many analysis centers derived from observations by VLBI, satellite laser ranging (SLR) to LAGEOS, lunar laser ranging (LLR), or GPS are combined into a homogeneous daily time series which is updated and distributed twice each week as *IERS Bulletin A*. Combined EOP values for the recent past are published together with predictions extending a year into the future.

In recent years, the *Bulletin A* polar motion results have been dominated by the precise determinations of the IGS combined Final products, with the Rapid series being used for the most recent measurements. The Rapid determinations are quite important for *Bulletin A* by providing timely, high-quality results which are most significant for polar motion predictions needed by real-time users. The recent accuracy of these series is estimated to be about 0.1 mas (per component) for the Finals and 0.2-0.3 mas for the Rapids. It is expected that implementation of the much more robust and improved terrestrial reference frame realization proposed by Kouba et *al.* (1998), where the coordinates and velocities of 47 sites are constrained to their ITRF96 values, will produce significantly more stable polar motion results. This, in turn, should improve the quality and reliability of current and near-term predictions of polar motion.

In addition to polar motion, *IERS Bulletin A* has become increasingly reliant on IGS estimates of length of day (LOD). The IGS started producing an official LOD product on 02 March 1997 using a weighted combination of LOD results submitted by each IGS Analysis Center (AC). To calibrate for LOD biases, each series is compared with the most recent 21 days of non-predicted UT1 values from *Bulletin A* (Kouba and Mireault, 1997; Ray, 1996). Shortly after its advent, the IGS combined LOD results were introduced into the *Bulletin A* combination to extend the UT 1 value of the most recent VLBI determination forward by integration. A few months later an independent set of GPS-based estimates of univeral time, derived at USNO and described below, were also included in *Bulletin A.* About two weeks of the most recent estimates are used, after calibration in offset and rate compared to overlapping UT 1 results from VLBI. These two series together have proven very successful in extending UT 1 results forward from the latest VLBI determinations, which may have a latency of up to about a week. As a consequence, the last non-predicted UT1 value in *Bulletin A is* now generally more accurate than 100 μs, usually considerably more so.

Errors in predicted EOP values are a significant source of systematic error in the IGS Predicted orbits, although they rarely dominate the overall error budget. Martin Mur *et al. (1998)* have stressed the need for improved EOP predictions for use in computing the IGS Predicted orbits. Partly to address this concern, refinements already under development were implemented in *Bulletin A* on 03 March 1998 (Ray and Luzum, 1998). The current and previous performance of the predicted polar motion variation is shown in Table 1. It can be seen that the improvement is most significant for the shortest prediction intervals (53% for 1 day) but dimishes over longer spans. Research is continuing into further improvements, which are likely to be implemented later in 1998.

For real-time users, given two updates of *Bulletin A* each week, the longest prediction interval is 7 days (for Tuesday updates compared with the previous Thursday issue which normally contains most recent data from 2 days earlier). This means that real-time users should experience polar motion errors no greater than about 2.4 mas (in an RMS sense per component). When the IGS delivery schedule for its Rapid products advances from 21:00 UTC to 16:00 UTC each day (by the end of 1998) this will allow each *Bulletin A* update to be performed during Washington afternoons with a reduced data latency of 1 day rather than the current 2 days. Thus the maximum prediction interval for real-time users will shorten to 6 days with an associated RMS polar motion error of about 2.0 mas. The *Bulletin A* update schedule could be changed to Monday/Thursday from the current Tuesday/Thursday to further reduce the maximum prediction interval to 5 days with an RMS polar motion error of about 1.7 mas. This has not been done in the past because most U.S. holidays occur on Mondays.

Table 1. Errors in *IERS Bulletin A* predictions for polar motion. The values tabulated are RMS scatters per component based on a retrospective analysis of actual polar motion variations during 1994- 1998.

predictions interval (days)	polar motion error (milliarcseconds)	
	previous	current
1	0.442	0.206
2	0.882	0.515
3	1.322	0.893
4	1.749	1.296
5	2.143	1.682
6	2.497	2.044
7	2.820	2.374
10	3.712	3,282
15	5.186	4.705

Predictions of UT1 variation are more problematic because the geophysical excitation is an order of magnitude larger than for polar motion. To reduce UT1 prediction errors will require very close coordination between the IGS and the IERS Sub-bureau, with heavy reliance on IGS Rapid LOD estimates and perhaps necessitating daily updates of *Bulletin A.*

As part of its contribution to the IGS, USNO prepares regular reports and plots of the performance of each IGS Analysis Center (AC) compared with *Bulletin A,* which are available at ht tp: //maia. usno. navy .mil/bullet in-a .html. Additional analysis reports are prepared occasionally to assess changes in IGS performance or to evaluate the geophysical implications (see for example Eubanks *et al.*, 1998).

IGS RAPID SERVICE ASSOCIATE ANALYSIS CENTER

Given the significance of the IGS results and our increasing reliance upon them, it is natural for USNO also to contribute actively as a data analysis center. Beginning 23 April 1997 USNO officially became a contributor to the IGS Rapid products. Originally we intented to eventually begin submitting Final and other products to become a full IGS AC. Since that time, however, other GPS-related activities have developed, such as the IGS/BIPM timing project (Ray, 1998), which are more closely tied to the US NO mission and therefore take higher priority. Given limited resources, USNO would, for the time being, prefer not to assume the additional responsibilities of a full AC. We suggest that the IGS recognize Rapid Service Associate Analysis Centers (RSAACs) as contributors of rapid service and prediction products. We plan to begin producing and contributing predicted GPS orbits during 1998.

An emerging interest at USNO is improved GPS orbits for a variety of real-time applications, including precise time transfer. This requires the highest quality Rapid and Predicted orbits and EOPs. These interests mesh naturally with full participation in the IGS/BIPM timing project. In support of this, US NO has already deployed a TurboRogue SNR12 receiver in Washington, DC connected to the USNO Master Clock (MC) as its

frequency reference. A second receiver is being deployed at Falcon Air Force Base in Colorado Springs, site of the USNO Alternate Master Clock (AMC) and the operations center for GPS. The MC and AMC are kept closely synchronized by regular two-way satellite time transfer (TWSTT) observations. These IGS sites can therefore serve as important comparison sites in the IGS/BIPM project.

Basic features of the USNO analysis strategy are summarized in Table 2. The software used is GIPSY/OASIS II, developed and maintained by JPL.

Table 2. USNO Analysis Strategy.

Software	GIPSY/OASIS II (vers. 4.8)
Observable	carrier phase & pseudo-range at 7.5 min.
Arc length	3+24 hr.
Network	30 global sites (usually)
Elevation cutoff	15 deg.
Sat. parameters	initial position & velocity, rad. pressure scale & Y-bias as constants, X,Z rad. pressure scales as stochastic
Attitude	yaw rates for eclipsing sats.

GPS DETERMINATIONS OF UNIVERSAL TIME

Elsewhere Kamrneyer (1998) has described his method to determine UT1 -like variations from an analysis of GPS orbit planes as estimated for IGS Rapid submissions. Briefly, the Earth-fixed GPS ephemerides determined operationally at USNO are compared to orbit planes propagated using a modeled radiation pressure acceleration normal to each orbit plane, For each satellite, the modeled acceleration is expressed relative to the projection of the Sun direction on the orbit plane and depends only on the angle from the orbital angular momentum to the Sun. The models being used were obtained empirically from observed experience when this angle was greater than 90° during 1994-1995. For each satellite, there is a unique axial rotation angle which brings the observed Earth-fixed positions into alignment with the propagated orbit plane. Since the propagated orbit plane of each satellite is different from its osculating orbit plane in an inertial frame, offsets are added to the rotation angles to form single-satellite estimates of GPS-based universal time. The median of these values for the 13 satellites modeled gives the UT estimate reported to *Bulletin A.*

Kammeyer's results show quite encouraging short-term performance. The relatively slow drifts allow sliding segments of these data to be including in the *Bulletin A* combination after calibration only for an offset and a rate. The residual scatter is about 75 μs over 3-week intervals. The procedure is described above and has proven very successful in extending more accurate but less timely VLBI measurements of UT1 to nearer real-time. Over longer spans these GPS-based determinations drift systematically, up to about 600 μs in six months.

Several improvements can be made. The long-term drifts reflect deficiencies in empirical models for the orbit plane motions. With the longer series of orbits now available, better models should be feasible. In particular, the present models are based

on data collected before the current yaw bias was implemented. Models can be constructed for all satellites, not just the 13 currently being used. The procedure could be applied to the more precise and reliable IGS combined orbits rather using the USNO orbits.

REFERENCES

Eubanks, T. M., J.R. Ray, and B .J. Luzum, The atmospheric excitation of rapid polar motions, *Eos Trans. American Geophysical Union,* in press 1998.

Kammeyer, P., Determination of a UT1-like quantity by comparing GPS positions to propagated orbit planes, in preparation 1998.

Kouba, J., and Y. Mireault, Analysis Coordinator report, in *International GPS Service for Geodynamics, 1996 Annual Report,* edited by J.F. Zumberge, D.E. Fulton, and R.E. Neilan, Jet Propulsion Laboratory, Pasadena, California, pp. 55-100, 1997.

Kouba, J., J. Ray, and M.M. Watkins, IGS reference frame realization, in 1998 *IGS Analysis Center Workshop Proceedings,* European Space Operations Centre, Darmstadt, Germany, (this volume), in press 1998.

Martín Mur, T. J., T. Springer, and Y. Bar-Sever, Orbit predictions and rapid products, in 1998 *IGS Analysis Center Workshop Proceedings,* European Space Operations Centre, Darmstadt, Germany, (this volume), in press 1998.

Ray, J., GPS measurement of length-of-day: Comparisons with VLBI and consequences for UT1, in *1996 IGS Analysis Center Workshop Proceedings,* edited by R.E. Neilan, P.A. Van Scoy, and J.F. Zumberge, Jet Propulsion Laboratory, Pasadena, California, pp. 43-60, 1996.

Ray, J, The IGS/BIPM time transer project, in 1998 *IGS Analysis Center Workshop Proceedings,* European Space Operations Centre, Darmstadt, Germany, (this volume), in press 1998.

Ray, J., and B. Luzum, Improved polar motion predictions, IGS Electronic Mail #1816, http://igscb.jpl.nasa.gov/igscb/mail/igsmail/igsmess. 1816, 27 Feb. 1998.

THE IGS REGIONAL NETWORK ASSOCIATE ANALYSIS CENTER FOR SOUTH AMERICA AT DGFI

Wolfgang H. Seemueller. Hermann Drewes
Deutsche Geodaetisches Forschungsinstitut (DGFI)
D-80539 Muenchen, **Germany**

INTRODUCTION

Early in 1996 the International GPS Service for Geodynamics (IGS) called for participation in a pilot project to densify the IERS Terrestrial Reference Frame (ITRF) by regional networks and a distributed data processing by Regional Network Associate Analysis Centers (RNAAC). DGFI is acting on behalf of the SIRGAS project (Sistema de Referencia Geocentric para America del Sur) as a RNAAC for South America. Beginning in mid of 1996 all available data of permanently observing GPS stations in the mainland of South America and surrounding regions are processed routinely and forewarned as SINEX files to the IGS Global Data Centers.

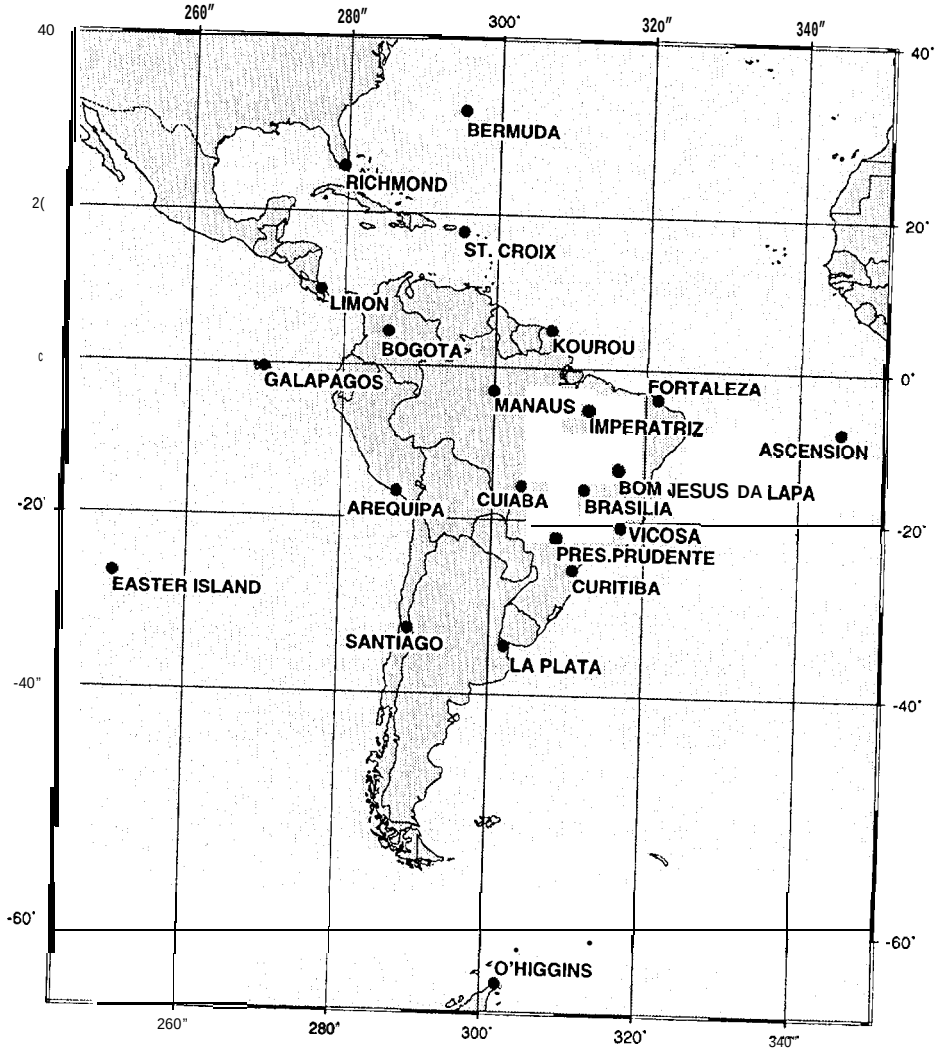

Fig. 1: Regional Network processed by RNAAC SIRGAS

SUMMARY

The RNAAC SIRGAS coordinate solutions are generated weekly using the Bernese Processing Engine (BPE version 4.0, Rothacher and Mervart, 1996), starting with the beginning of the pilot project to densify the IERS Terrestrial Reference Frame (ITRF) in June 1996. The regional network consists of 22 GPS stations (fig. 1), seven of nine Brazilian GPS stations are processed by RNAAC exclusively.

Conclusions from the analysis are

- **Note: the vertical scale of the figures is 20 cm normally, except when the variations are bigger; then you see a mark that the scale differs.**

- **Posters 1 to 3 are the original posters shown in Darmstadt, they are reduced from DIN AO to DINA4, and therefore they are not very nicely readable.**

- **To have a clearer insight to the discrepancies all comparisons for all stations are shown on one page each (figures 2 to 10)**

- **A rough analysis of processing results is demonstrated in the figures 2 to 10. We show the deviations in North, East and Up components of selected stations for the internal consistency (variations of weekly SIR R solutions with respect to the first solution), the diurnal variations of RNAAC solutions with respect to the first solution (only for problematic periods), and the external consistency by comparison of SIR R SINEX with the GNAAC'S P-Sinex solutions (after Helmert transformation because the SIR R-SINEX solutions are free network solutions).**

- **The deviations are typically in the sub-centimeter level for horizontal components and in the 1 to 2 cm level for the vertical (see Fig. 8 and 9). The small deviations of the seven Brazilian exclusive RNAAC SIRGAS stations (see e.g. Fig. 10, station President Prudente) are due to the fact that no other Analysis Center is processing these data, i.e. only the RNAAC SIRGAS solution is included in the "combination".**

- **Figures 2 to 7 show the deviations for IGS stations with problematic periods only. For GPS week 910 to 920 the deviations between the SIR R solutions and the GNAAC polyhedron solutions from Newcastle University increase, but this is not valid for the comparison with the MIT solutions. This is the case especially for station Limon (Fig.2), Arequipa, Ascension and Santiago de Chile (Fig. 5 to 7). The diurnal variations of SIR R solutions don't figure out this abnormal behaviour. The GNAAC Newcastle will solve this problem**

- **Station Limon/Costa Rica shows a jump in the Up component of about +90 cm from day 97305 to 97306 (Fig.2). Nothing is reported in the IGSMAIL about a change. The reason for this discontinuity is unknown.**

- **The Up component of station Kourou (Fig.3) is strongly varying in the daily solutions, this valid for the weekly solutions also.**

REFERENCE

Rothacher, M. and Mervart, L. (eds.): Bernese GPS software 4.0. Astronomical Institute, University of Berne, 1996.

IGS STATION LIMON

Variations of weekly SIR R solutions with respect to first solution

variations of daily SIR R solutions with respect to first solution

Comparison of diff. SIR R and GNAAC P after Helmert transf.

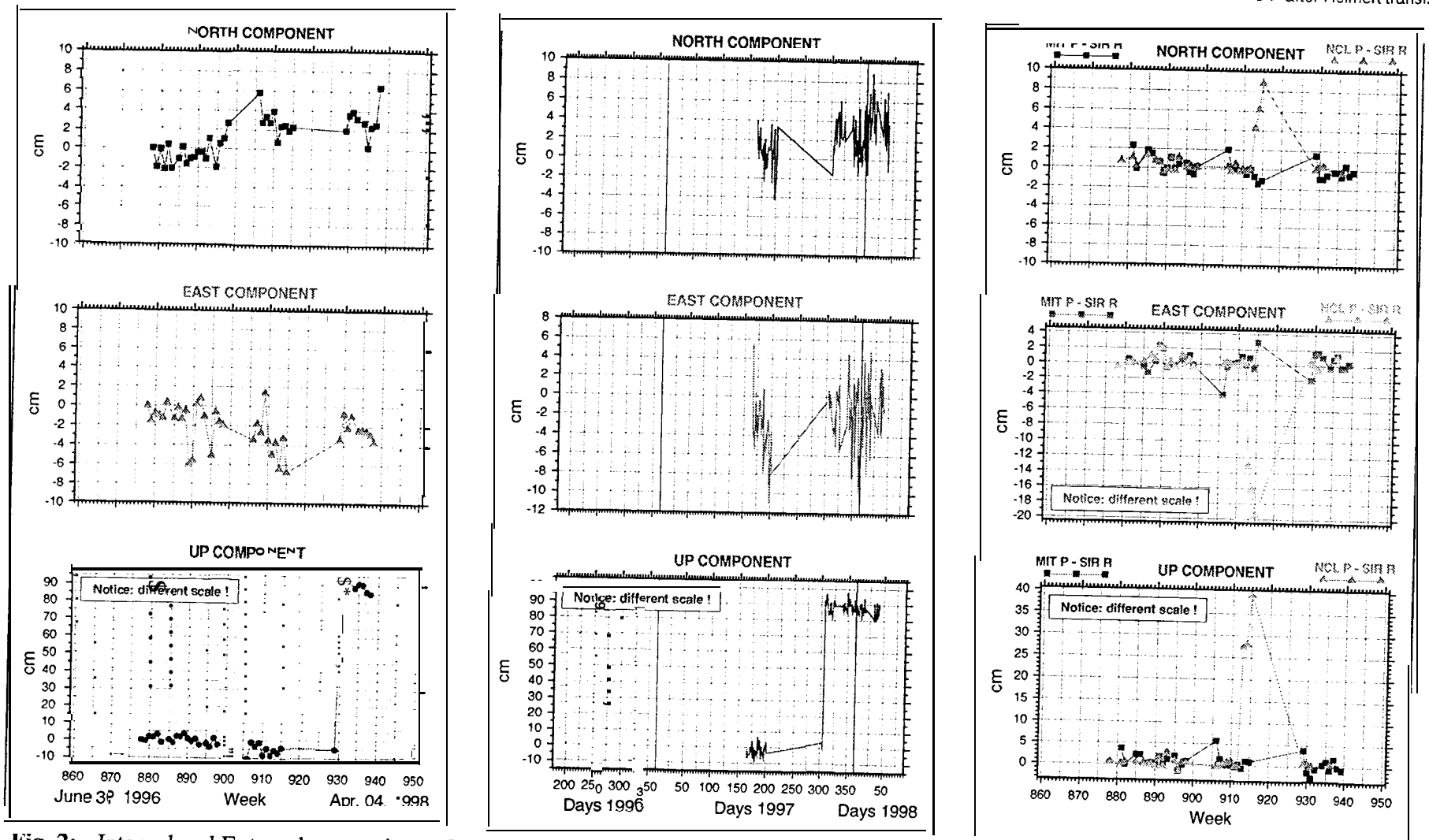

Fig. 2: Internal and External comparison of RNAAC SIR solutions (Station Limon)

IGS STATION KOUROU

Variations of weekly SIR R solutions with respect to first solution

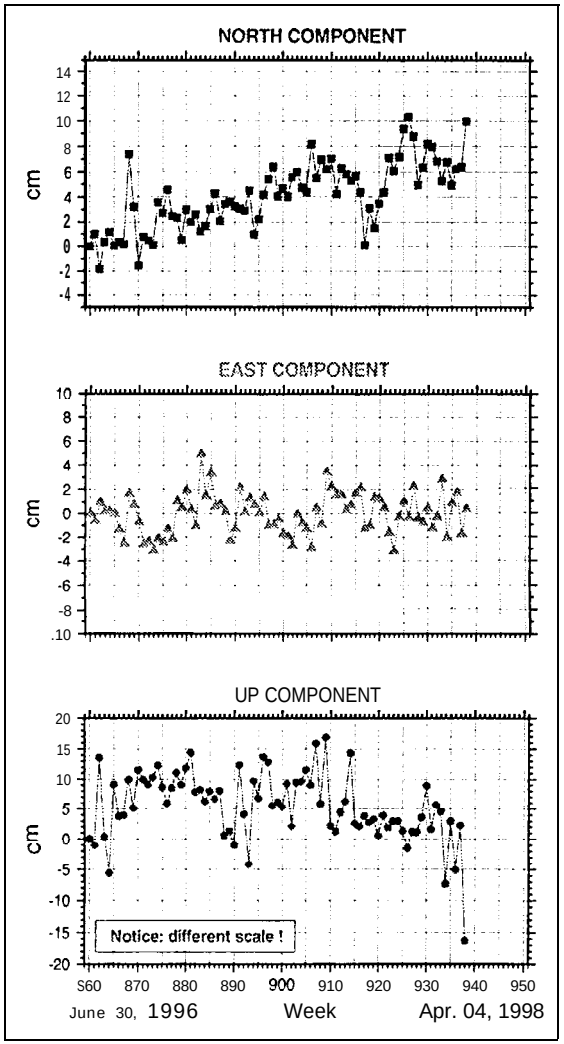

Variations of daily SIR R solutions with respect to first solution

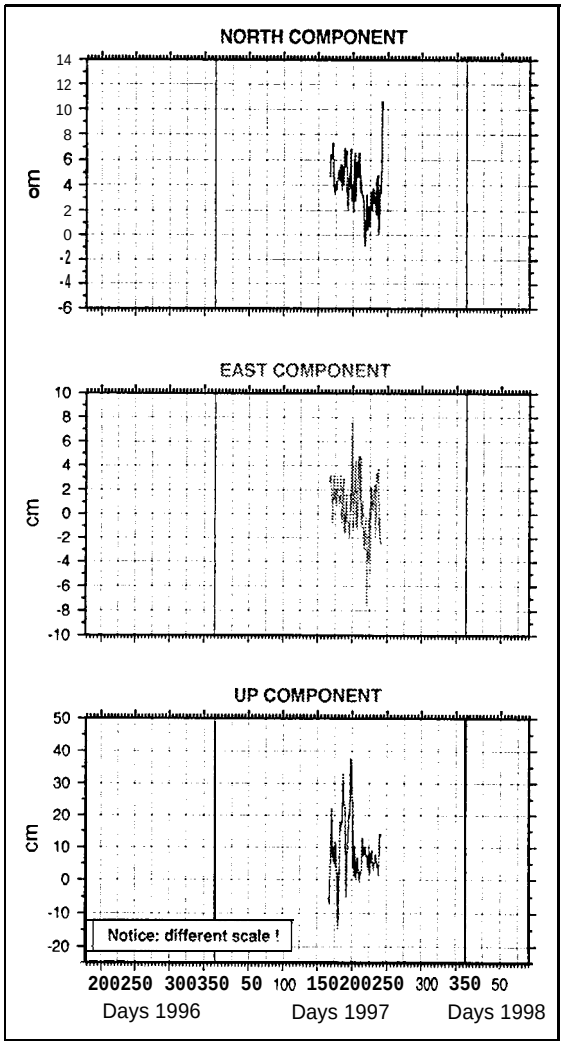

Comparison of cliff. SIR R and GNAAC P after Helmert transf.

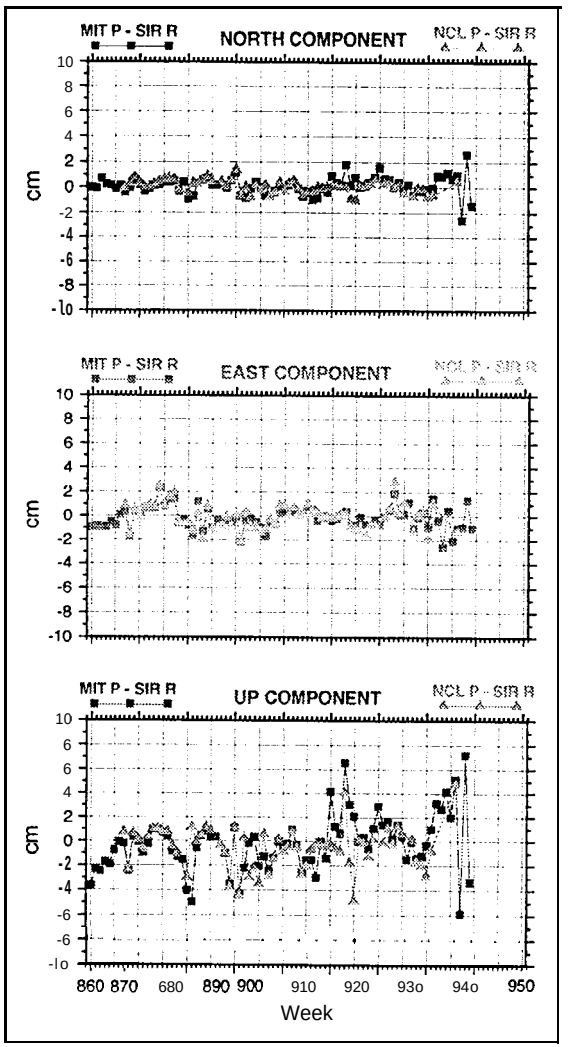

Fig. 3: Internal and External comparison of RNAAC SIR solutions (Station Kourou)

IGS STATION ST. CROIX

Variations of weekly SIR R solutions with respect to first solution

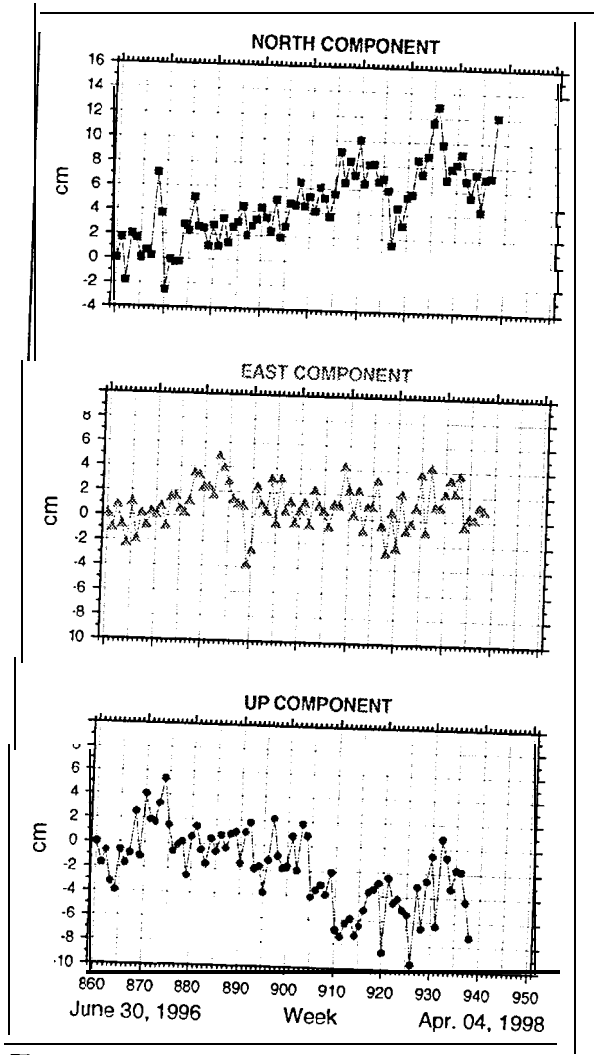

Variations of daily SIR R solutions with respect to first solution

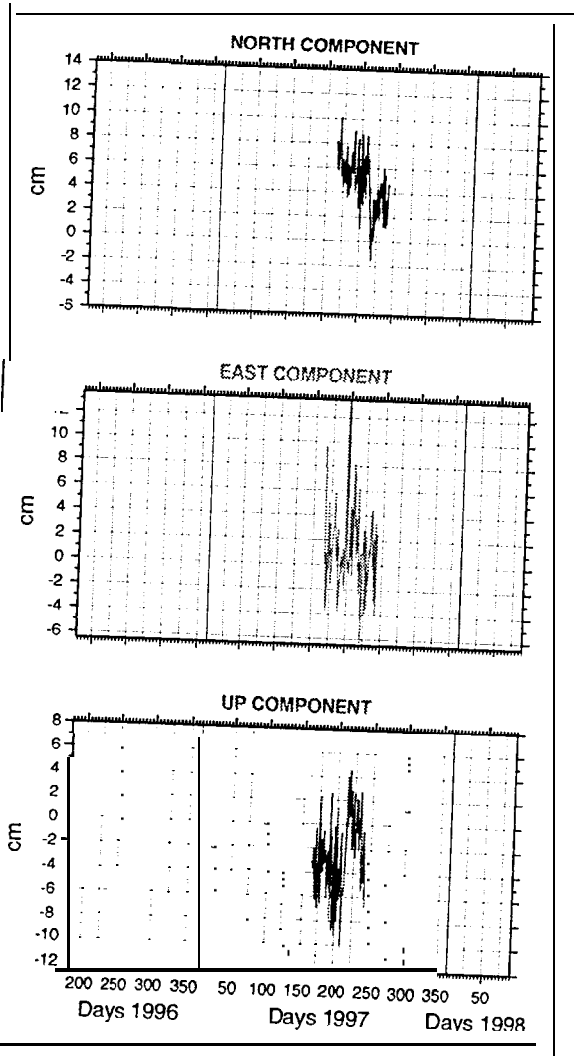

Comparison of diff. SIR R and GNAAC P after Helmert transf.

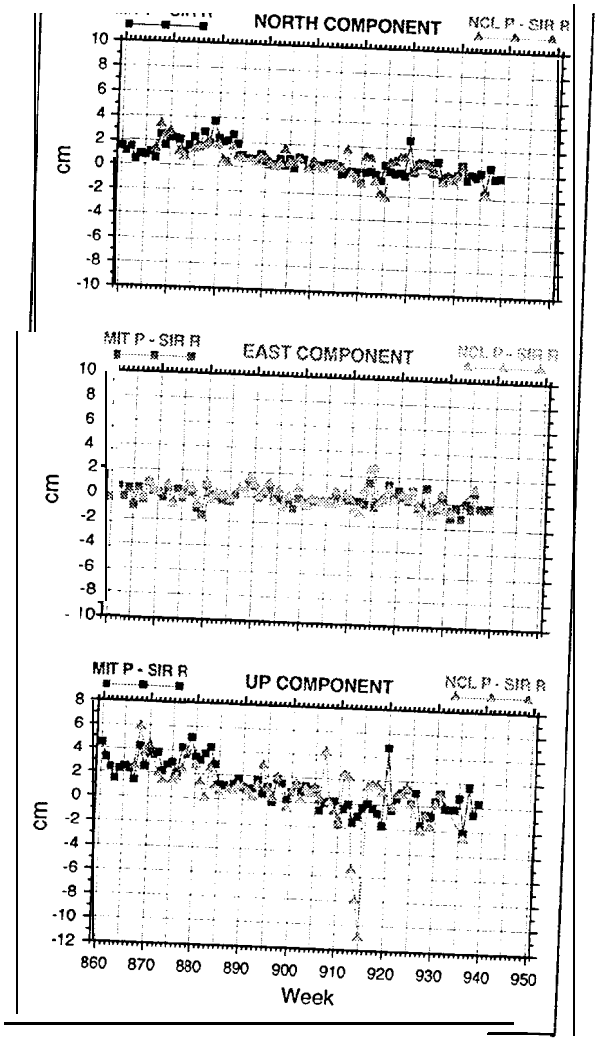

Fig. [illegible] External comparison of RNAAC SIR solutions (Station St. Croix)

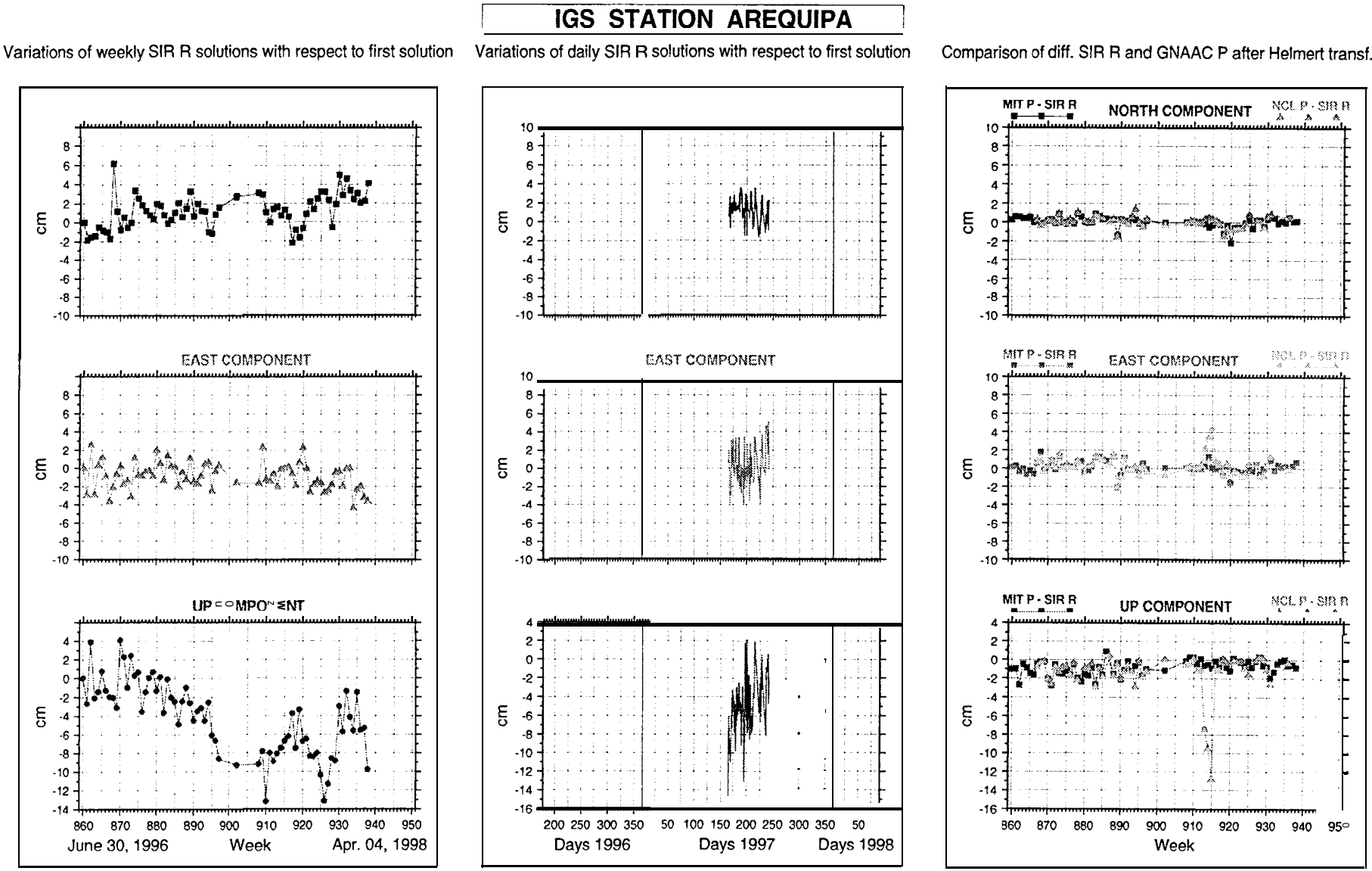

Fig. 5: Internal and External comparison of RNAAC SIR solutions (Station Arequipa)

IGS STATION SANTIAGO

Variations of weekly SIR R solutions with respect to first solution

Variations of daily SIR R solutions with respect to first solution

Comparison of cliff. SIR R and GNAAC P after Helmert transf.

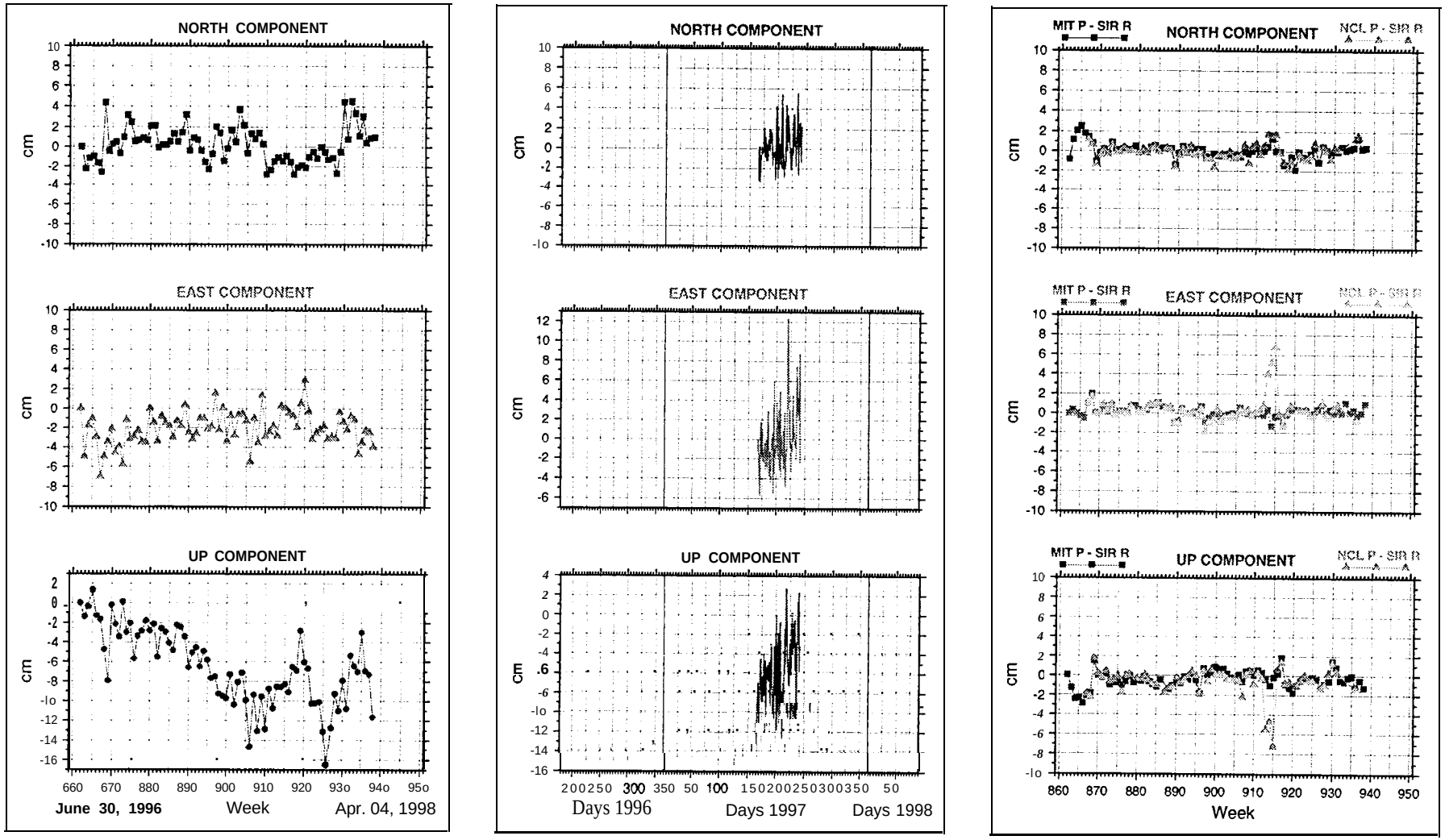

Fig. 6: Internal and External comparison of RNAAC SIR solutions (Station Santiago de Chile)

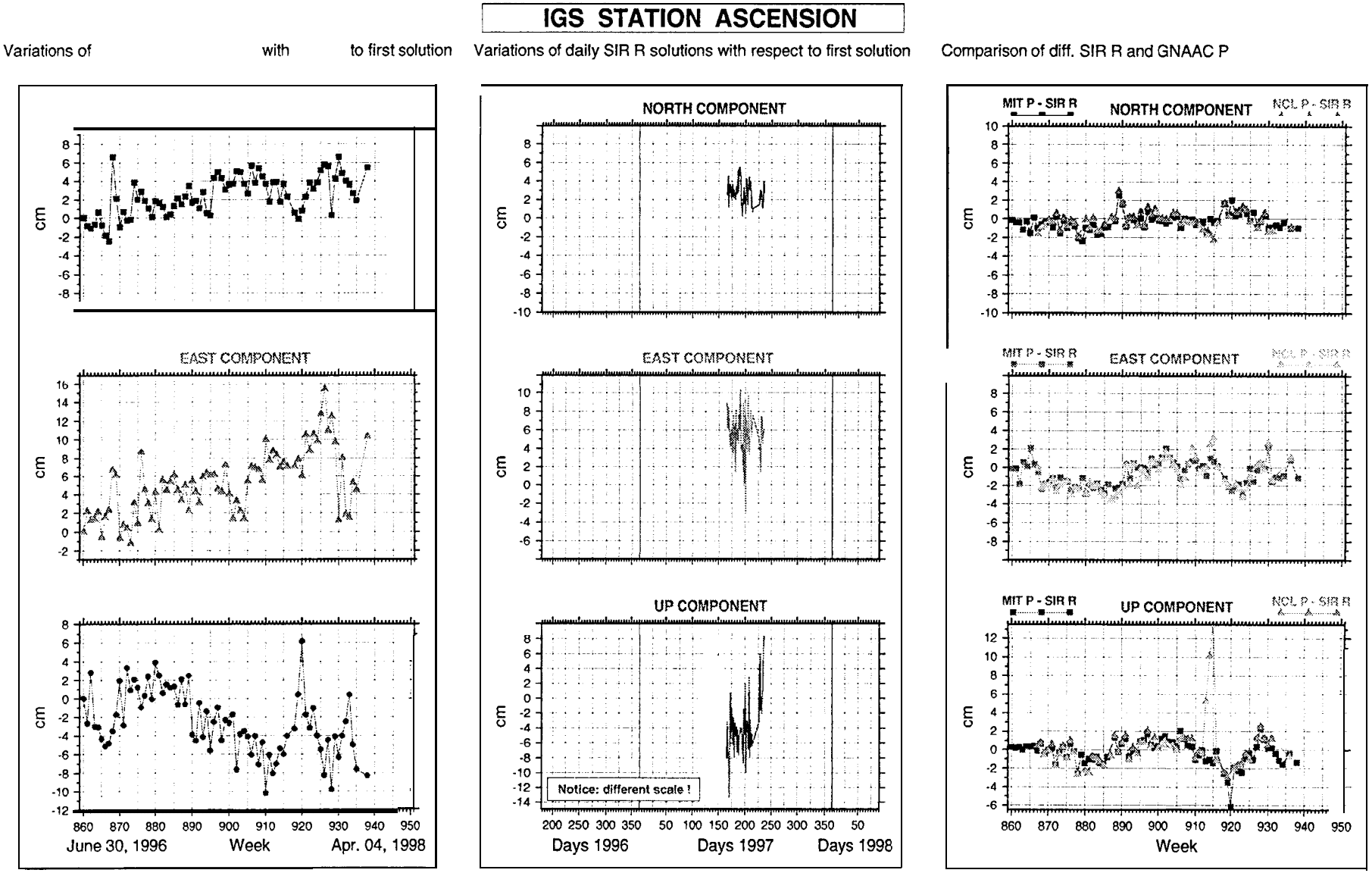

Fig. 7: Internal and External comparison of RNAAC SIR solutions (Station ASCENSION)

IGS STATION BRASILIA

Variations of weekly SIR R solutions with respect to first solution

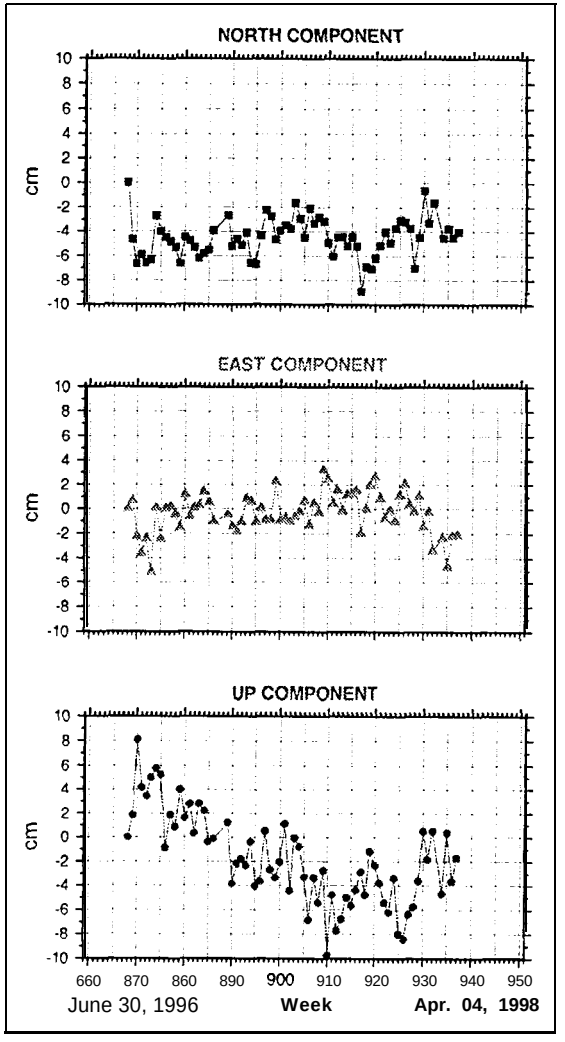

Variations of daily SIR R solutions with respect to first solution

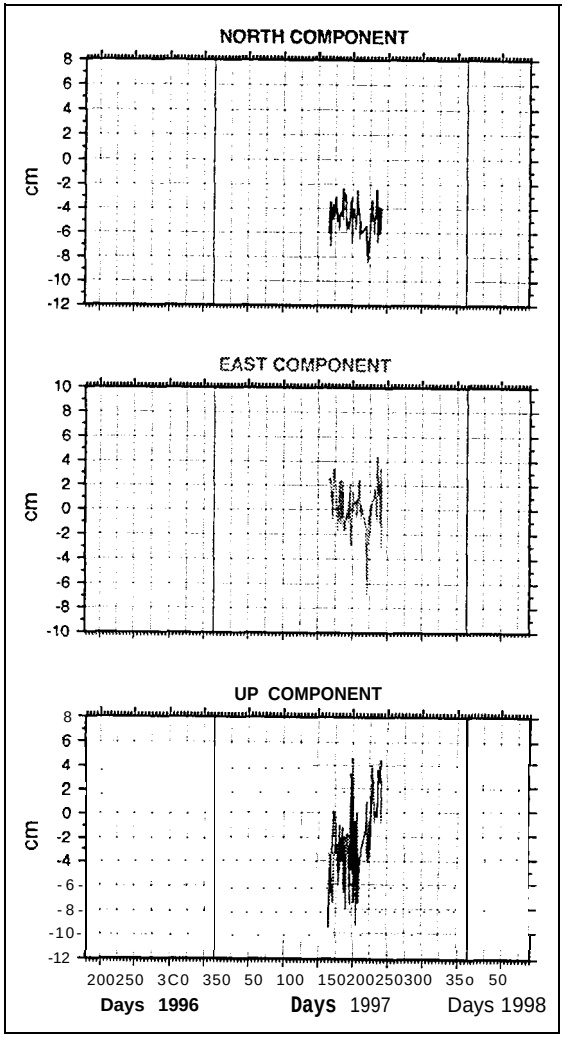

Comparison of cliff. SIR R and GNAAC P after Helmert transf.

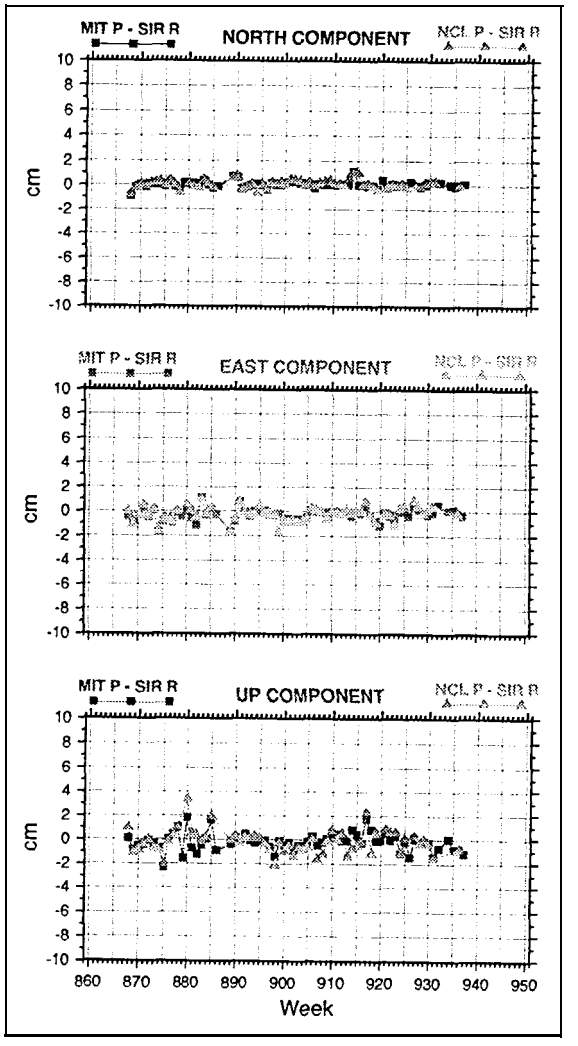

Fig. 8: Internal and External comparison of RNAAC SIR solutions (Station Brasilia)

IGS STATION FORTALEZA

Variations of weekly SIR R solutions with respect to first solution

Variations of daily SIR R solutions with respect to first solution

Comparison of diff. SIR R and GNAAC P after Helmert transf.

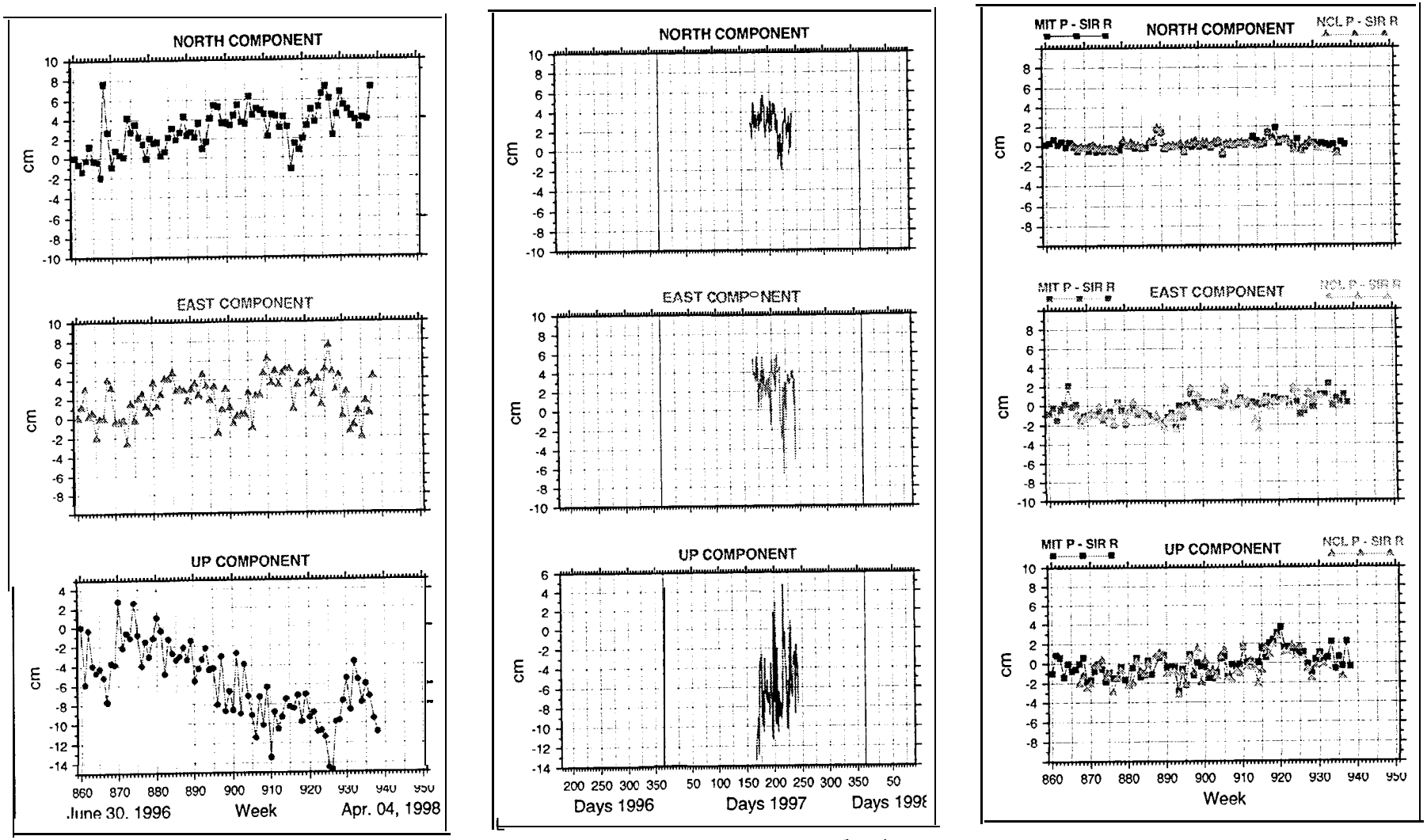

Fig. 9: Internal and External comparison of RNAAC SIR solutions (Station Fortaleza)

STATION PRESIDENT PRUDENTE

Variations of weekly SIR R solutions with respect to first solution

Variations of daily SIR R solutions with respect to first solution

Comparison of cliff. SIR R and GNAAC P after Helmert transf.

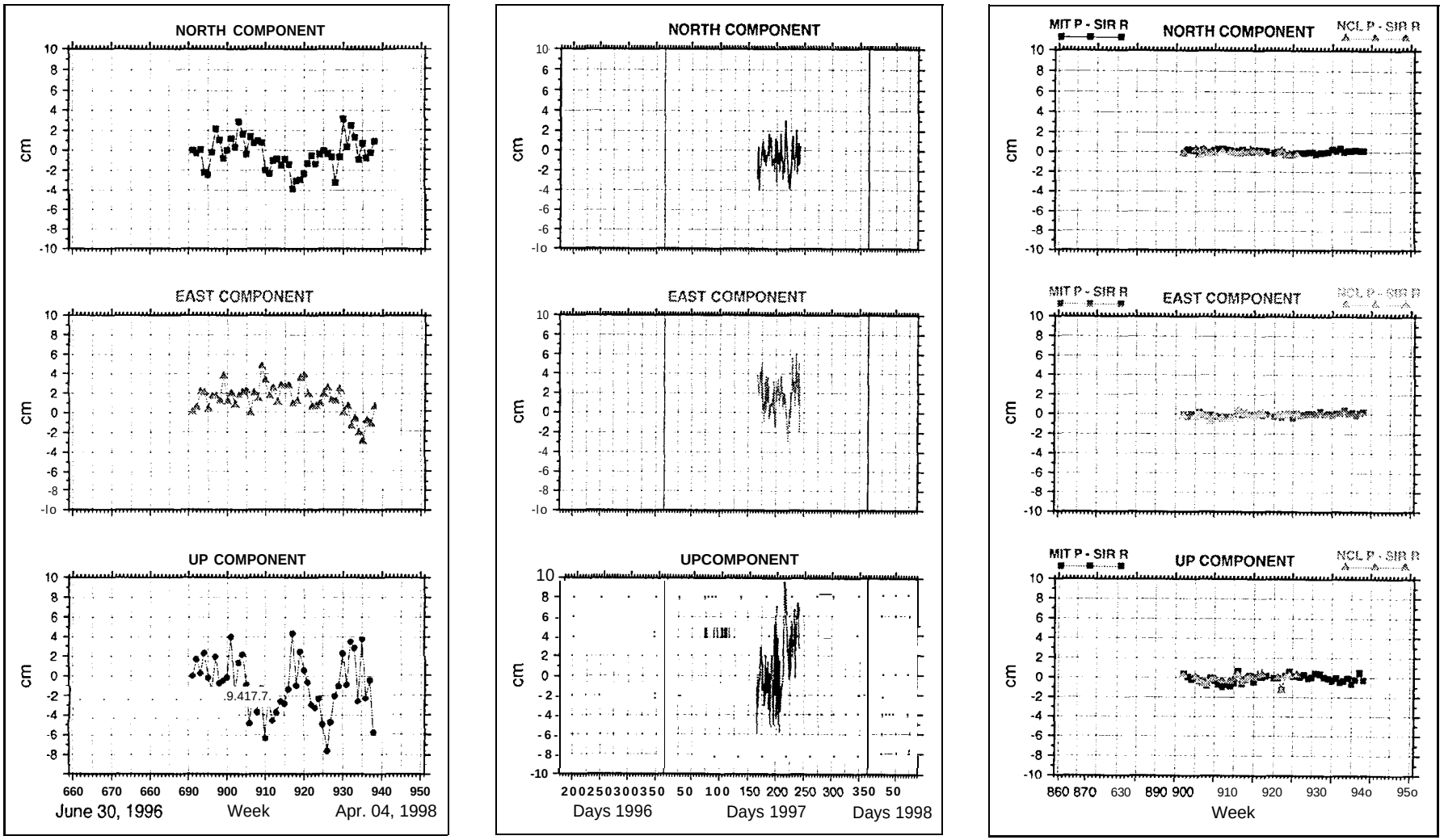

Fig. 10: Internal and External comparison of RNAAC SIR solutions (Station Presidente Prudence)

IGS Regional Network Associate Analysis Center SIRGAS
(**IGS** RNAAC SIR)

Brazilian GPS Stations

Internal Consistency of **RNAAC** SIR **Weekly** Solutions
Variations of Weekly SIR R Solutions with respect to the first Solution

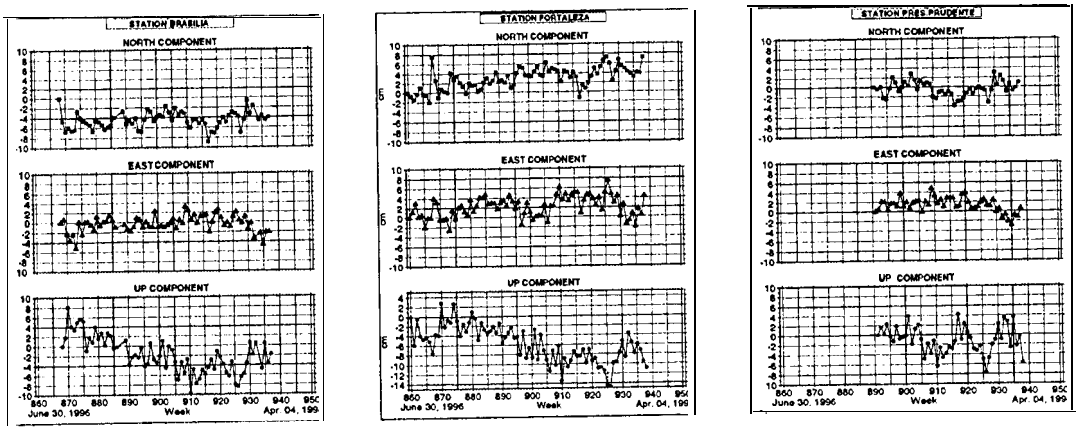

Diurnal Variations of **RNAAC** SIR Solutions
Variations of Daily SIR R Solutions with Respect to the first Solution

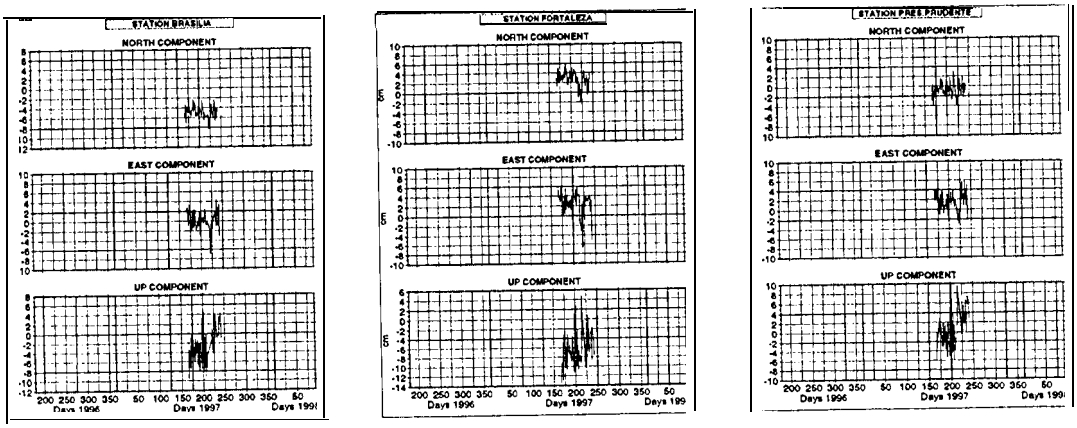

Comparison of **SIR R-SINEX** with **GNAAC's P-SINEX** Solutions
Differences in North, East ● d Up Components after Helmert Transformation

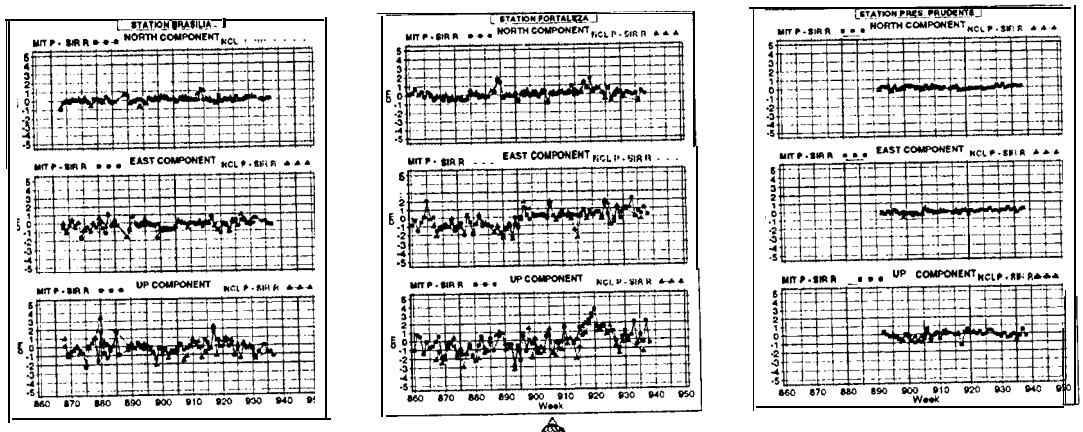

Poster 1: Selected Brazilian GPS Stations

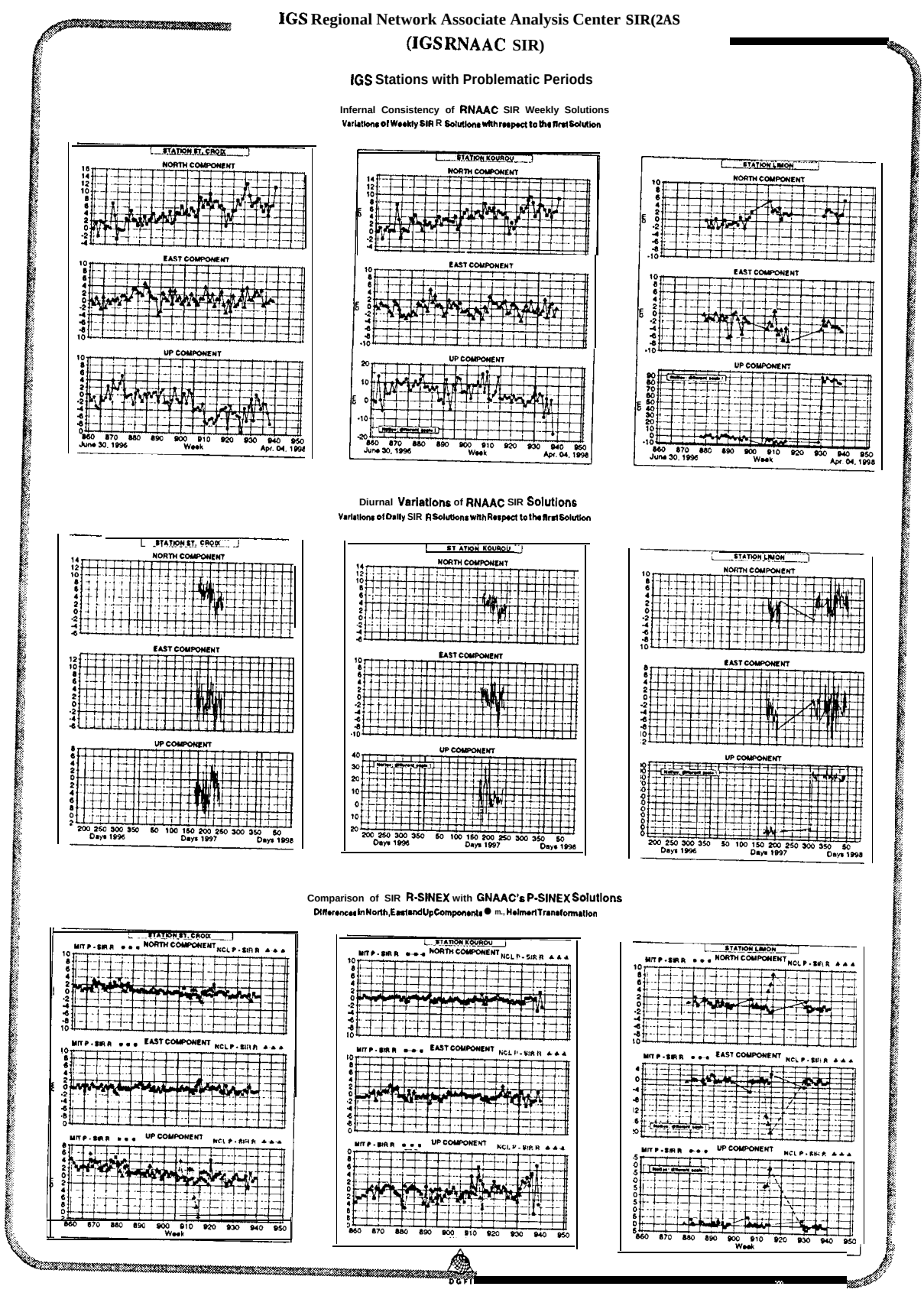

Poster 2: IGS Stations with Problematic Periods

IGS Regional Network Associate Analysis Center SIRGAS
(IGS RNAAC SIR)

IGS Stations with Problematic Periods

Internal Consistency of RNAAC SIR Weekly Solutions
Variations of Weekly SIR R Solutions with respect to the first Solution

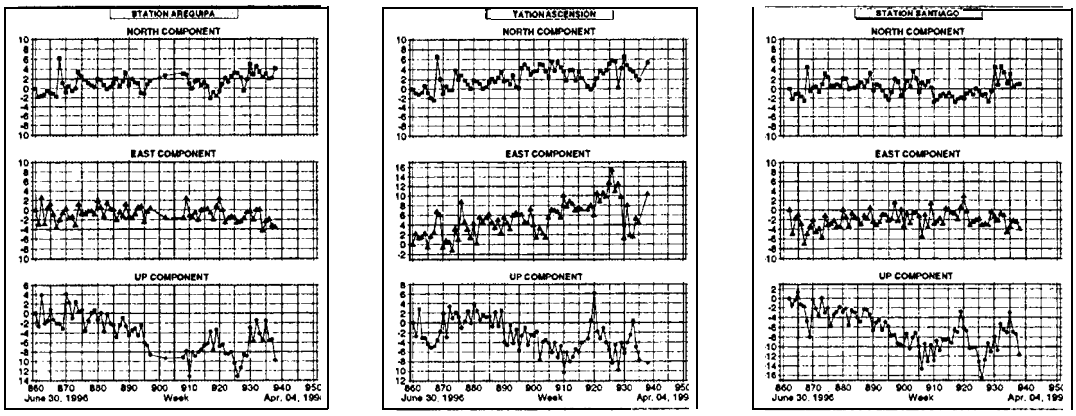

Diurnal Variations of RNAAC SIR Solutions

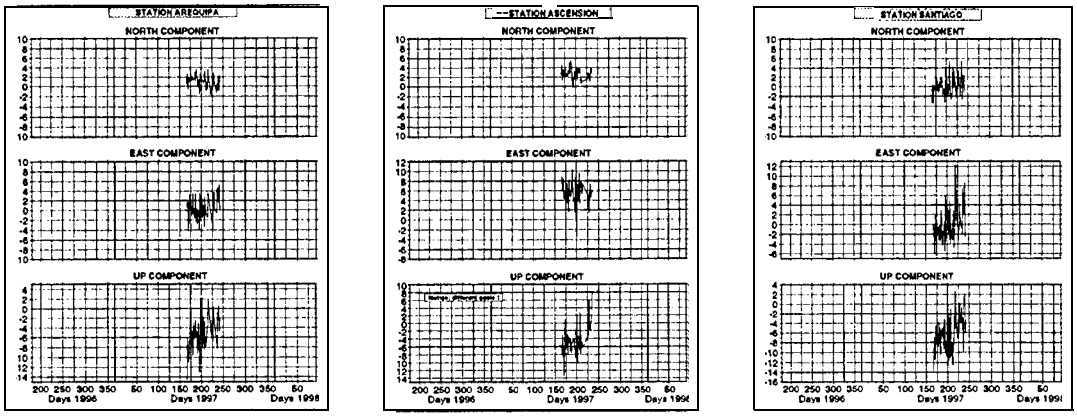

Comparison of SIR R-SINEX with GNAAC's P-SINEX Solutions
Differences in North, East and Up C m - a n . , Helmert Transformation

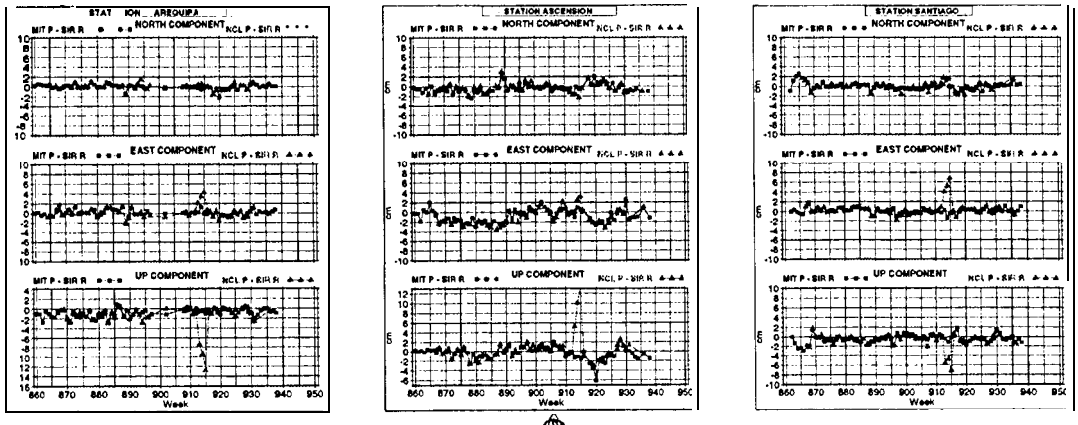

Poster 3: IGS Stations with Problematic Periods

THE NEWCASTLE GLOBAL NETWORK ASSOCIATE ANALYSIS CENTRE

Ra 'ed Ka war, Geoffrey Blewitt, and Phil Davies[†]

Department of Geomatics, University of Newcastle upon Tyne, UK

ABSTRACT

The Newcastle (NCL) GNAAC has been operational for two years. It produces weekly combined solutions for the GNET, and the PNET (i.e., densified GNET); based on the ACS and RNAACs data respectively. In our poster at this workshop, we present the current status of the NCL GNAAC, summary of data submission and analysis, strategies, and some of the weighted RMS postfit residuals of the AC solutions with respect to the NCL GNAAC solutions.

INTRODUCTION

The Newcastle Global Network Associate Analysis Center (NCL GNAAC) was established in 1995 as a response to the call for participation in the pilot project of the IGS distributed processing scheme for the densification of the ITRF. This scheme has two components: the combined analysis (G-SINEX) of the Analysis Centers' coordinate solutions (A-SINEX); and the integration (P-SINEX) of regional network submissions (R-SINEX). The NCL GNAAC commenced producing coordinate weekly combined solution files, G-SINEX, from GPS week 817. Since GPS week 0834 the NCL GNAAC started to include station discrepancy information for each Analysis Center. With regard to the P-SINEX component, this started in year 1996.

NCL GNAAC STATUS

In November 1997 and due to the change over of the NCL GNAAC operator; there were some reports not retrieved from both the GNET and the PNET. The GNET

[†] Currently at Ordnance Survey, Southampton, UK

reports were all recovered and routine operation started again. With respect to the PNBT report we are still working on that.

SUMMARY OF DATA SUBMISSION AND ANALYSIS

As **previously mentioned we analyze data from ACS and RNAACs. Figure 1 shows a bar diagram for the sources of the A-SINEXS that we analyze. It seem fairly obvious** that most of the ACS have been submitting data to the CDDIS on time. Figure 2 shows that the NCL GNAAC should be routinely analyzing solutions from 6 RNAACs: AUS, GIA, PGC, GSI, SIR and EUR. However, this is not the case, solutions from only three or four RNAACS are being analyzed routinely. There are two reasons behind this: the first, and most important is that the RNAACS are not submitting data to the CDDIS on time; and the second is caused by our recent strategy to analyze only the stations that have a formal log file at the IGS CB (see next section).

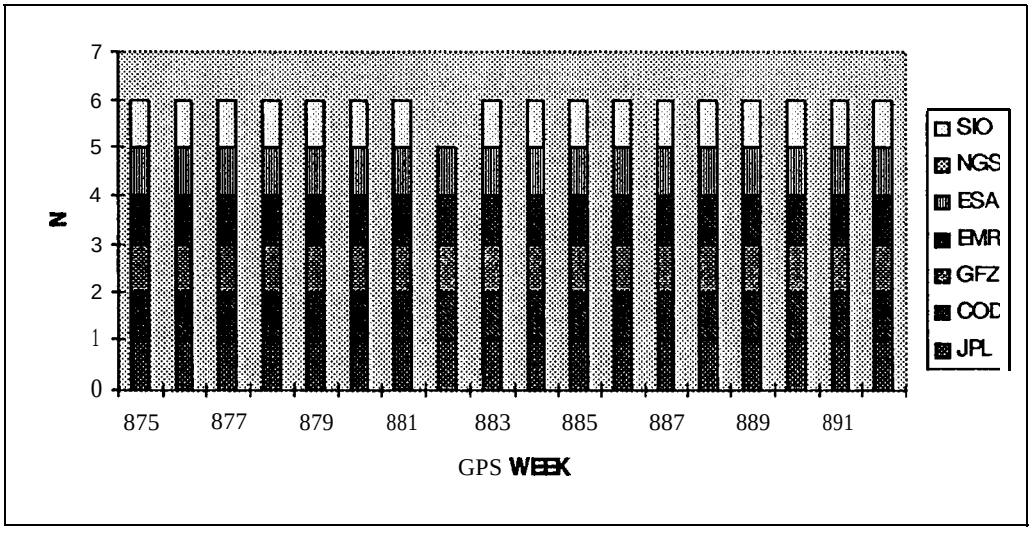

Figure 1: The number and sources of A-SINEX data analysed.

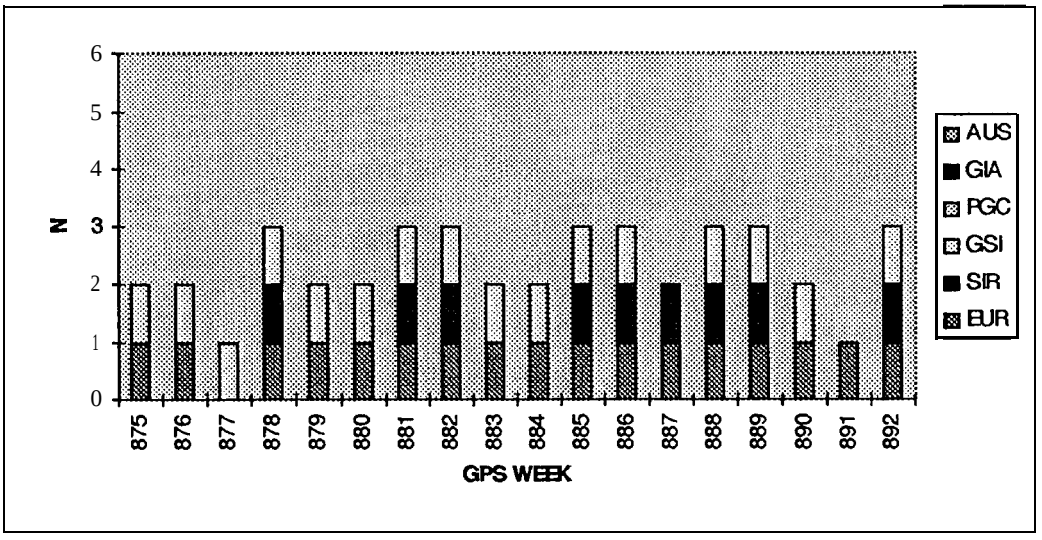

Figure 2: The number and sources of A-SINEX data analysed.

STRATEGY

Since October 1997 an automatic catalogue update system has been put in place at NCL. This system downloads theloghist.txt file, maintained bythe IGS CB, and create history SINEX file that is used for station information. The adoption of this policy means that there will be no discrepancy of the history block at A- & P-SINEX, and only stations that have official log files will be analyzed. Consequently, many stations have been thrown away out of our analysis, and sometime all of an RNAAC'S data are rejected as a result of this.

RESULTS

Figure 3 shows the Weighted Root Mean Square (WRMS) in mm for the postfit residuals, from the A-SINEX to the NCL G-SINEX. It is noticed that the maximum value is about 25 mm of the postfit residuals which emphasizes the importance of combining the A-SINEXs to one solution.

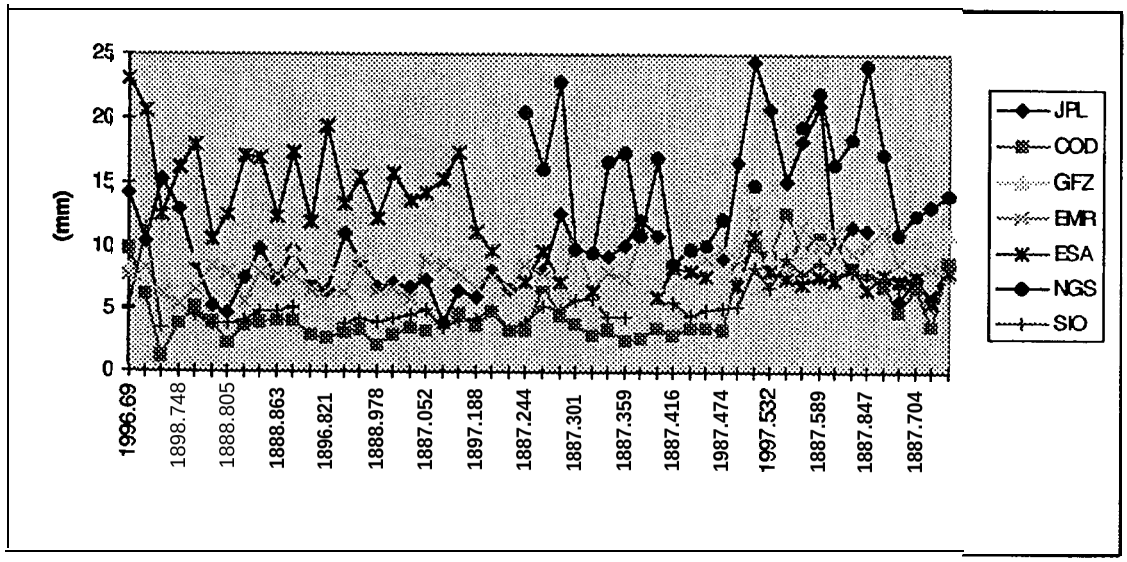

Figure 3: Post-fit residuals' weighted RMS (mm) (A-SINEXs to NCL G-SINEX).

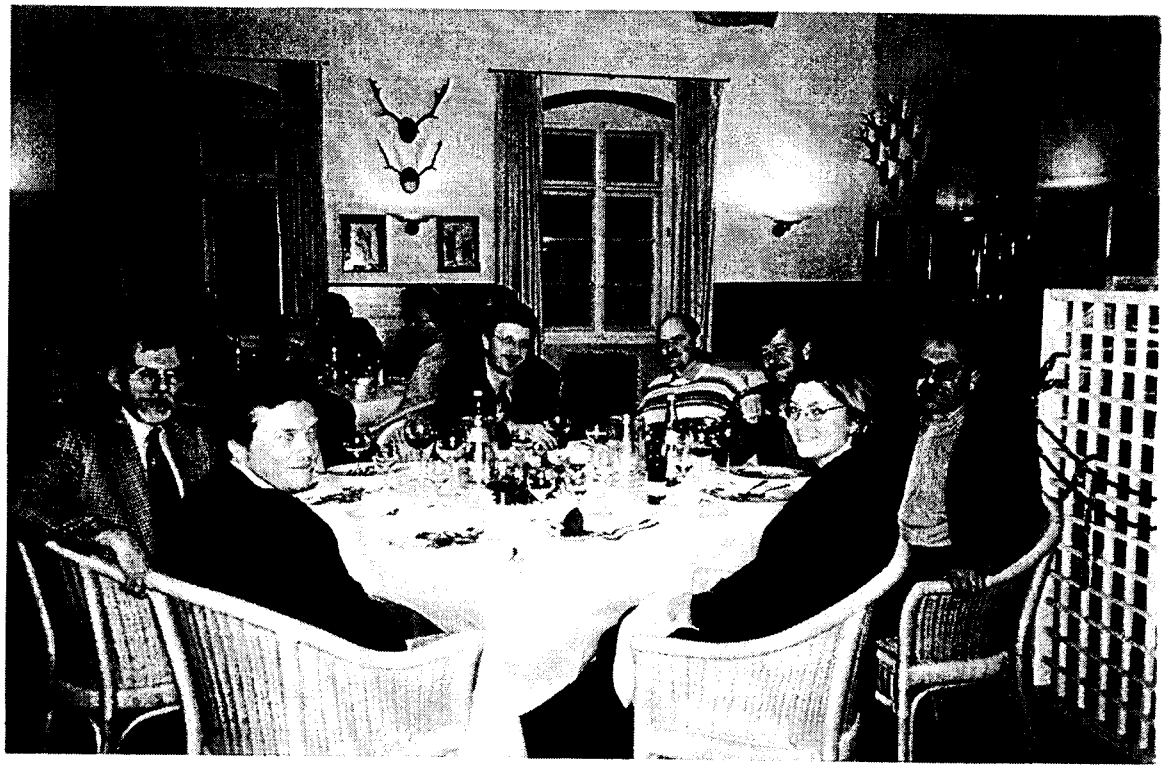

IGS Workshop Dinner, Jagschloss Kranichstein, Darrnstadt, 10 February 1998.
(Photos courtesy of Ruth Neilan, JPL.)